Quantum networks based on color centers in diamond

Ruf, Maximilian; Wan, Noel H.; Choi, Hyeongrak; Englund, Dirk; Hanson, Ronald

DOI
10.1063/5.0056534

Publication date
2021

Document Version
Final published version

Published in
Journal of Applied Physics

Journal of Applied Physics PERSPECTIVE scitation.org/journal/jap

Quantum networks based on color centers in diamond

Cite as: J. Appl. Phys. **130**, 070901 (2021); doi: 10.1063/5.0056534
Submitted: 11 May 2021 · Accepted: 16 July 2021 ·
Published Online: 16 August 2021

Maximilian Ruf,[1,2] Noel H. Wan,[3,4] Hyeongrak Choi,[3,4] Dirk Englund,[3,4,5,a)] and Ronald Hanson[1,2,a)]

AFFILIATIONS

[1]QuTech, Delft University of Technology, P.O. Box 5046, 2600 GA Delft, The Netherlands
[2]Kavli Institute of Nanoscience Delft, Delft University of Technology, P.O. Box 5046, 2600 GA Delft, The Netherlands
[3]Department of Electrical Engineering and Computer Science, Massachusetts Institute of Technology, Cambridge, Massachusetts 02139, USA
[4]Research Laboratory of Electronics, Massachusetts Institute of Technology, Cambridge, Massachusetts 02139, USA
[5]Brookhaven National Laboratory, Upton, New York 11973, USA

Note: This paper is part of the Special Topic on Materials, Methods, and Applications of Color Centers with Accessible Spin.
[a)]**Authors to whom correspondence should be addressed:** englund@mit.edu and r.hanson@tudelft.nl

ABSTRACT

With the ability to transfer and process quantum information, large-scale quantum networks will enable a suite of fundamentally new applications, from quantum communications to distributed sensing, metrology, and computing. This Perspective reviews requirements for quantum network nodes and color centers in diamond as suitable node candidates. We give a brief overview of state-of-the-art quantum network experiments employing color centers in diamond and discuss future research directions, focusing, in particular, on the control and coherence of qubits that distribute and store entangled states, and on efficient spin–photon interfaces. We discuss a route toward large-scale integrated devices combining color centers in diamond with other photonic materials and give an outlook toward realistic future quantum network protocol implementations and applications.

I. INTRODUCTION

With the Panama-Pacific International Exposition of 1914 fast approaching, AT&T's leadership grew increasingly alarmed: it was still impossible to hold a coast-to-coast telephone call, despite the company touting it for years. The essential problem "was a satisfactory telephone repeater," recalled an AT&T senior manager from conversations with the company's chief engineer John J. Carty.[1] Whereas mechanical repeaters adequately boosted voice signals on the metro-scale, they added so much noise that signals quickly became unintelligible over longer distances. A fundamentally new repeater technology was needed. Tasked with this urgent mission, Bell Laboratories developed the "audion" trion vacuum tube, just in time for the 1914 Exposition. Over the ensuing decades, the triode made way to the transistor, copper wires yielded to optical fiber, and binary digits ("bits") became the universal language of information, transcending physical modality. Today, as the authors edit these sentences over a globe-spanning video conference, the world is at the cusp of the next information revolution, as quantum bits ("qubits") have become the universal units fueling a new generation of "quantum information technologies." Once again, an essential challenge is to develop a "satisfactory repeater"—this time, capable of relaying (but not amplifying[2]) *quantum information* signals. This article provides a perspective on the progress toward one such "quantum repeater" as well as other quantum network technology using color centers in diamond to connect quantum information among spins and photons.

II. A BRIEF INTRODUCTION TO QUANTUM NETWORKS

In a future quantum network (see Fig. 1), remote parties are connected by sharing long-lived entangled states.[3,4] Arguably, the most promising way of linking distant nodes is to employ fiber- or free-space photonic communication channels to

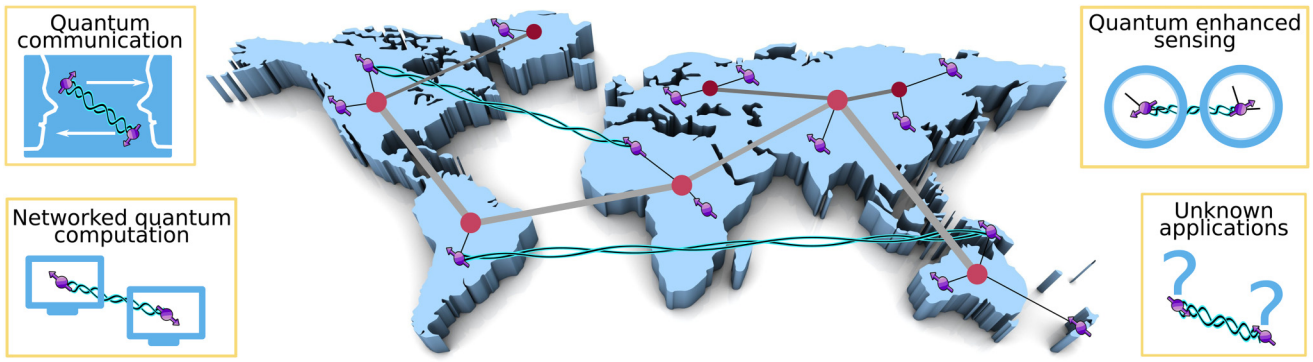

FIG. 1. Schematic overview of a future large-scale quantum network, consisting of nodes containing optically interfaced qubits (purple) with long coherence times. Photons routed via optical fibers or free-space channels serve as mediators to create entanglement (blue wiggled lines). Local area and trunk backbone quantum repeaters (dark and light red circles, respectively) are used to enable a high entanglement generation rate over large distances, overcoming photon transmission loss. The entanglement generation is heralded, meaning that detection of certain photon statistics signals the successful generation of an entangled state that is available to a network user for further processing and applications such as networked quantum computation, quantum secured communication, quantum enhanced sensing, and potential not yet discovered tasks.

establish entanglement. While all photon-based schemes are associated with losses that scale with distance,[5] motivating the need for quantum repeaters,[6] heralding entanglement generation on successful photon transmission events maps these losses into reduced entanglement generation rates without lowering entanglement fidelities.[7–9]

Optically mediated remote entanglement of individually controllable qubits has been generated for different materials platforms, including quantum dots,[10,11] trapped ions,[12–14] neutral atoms,[15–18] and nitrogen-vacancy (NV) centers in diamond.[19,20] Other promising systems, including so-called group-IV defects in diamond,[21–24] defects in SiC,[25–29] and rare-earth ions in solid-state hosts,[30–32] show great potential for quantum network applications, although remote entanglement has not yet been generated. Another less explored approach is to link distant superconducting quantum processors using the coherent conversion of microwave photons to telecom frequencies.[33–37]

Apart from fundamental tests of physics,[20] small-scale quantum networks have been used to demonstrate key network protocols such as non-local quantum gates,[17] entanglement distillation,[38] and very recently entanglement swapping.[39] These networks are currently limited to a few nodes,[39] distances of up to one kilometer,[20] and entanglement generation rates in the Hz to kHz regime.[10–16,19,20] A major challenge for the coming decade is to transition from the current proof-of-principle experiments to large-scale quantum networks for use in fields such as distributed quantum computation,[40,41] quantum enhanced sensing,[42,43] and quantum secure communication.[44]

In this Perspective article, we focus on color centers in diamond as potential building blocks for large-scale quantum networks. We identify their strengths and challenges, current research trends, and open questions, with a focus on qubit control, coherence, and efficient spin–photon interfaces. We lay out a path toward large-scale, integrated devices and discuss possible protocols and functionalities such devices could enable.

This article is organized as follows: Sec. III introduces the requirements for the nodes of a quantum network and gives a high-level overview of why color centers in diamond are promising candidates to meet these demands. We then give a brief overview of state-of-the-art quantum network experiments employing color centers in diamond in Sec. IV to give the reader a sense of the current research status. In Sec. V, we introduce the physics behind color centers in diamond, to understand their strengths and challenges for quantum network applications in the remainder of this article. Section VI discusses open questions regarding the coherence and control of nuclear spin memory qubits surrounding color centers in diamond that can be used as additional quantum resources. In Sec. VII, we outline the need and strategies for an enhancement of the spin–photon interface of diamond color centers and discuss promising future research in this direction. Section VIII outlines a path toward large-scale, integrated diamond devices that may enable future quantum network experiments with high rates. Finally, Sec. IX concludes by illuminating possible applications for future quantum networks.

III. REQUIREMENTS FOR A QUANTUM NETWORK NODE

To make a material platform suitable for a node in a quantum network in which entanglement is mediated by photons, it has to fulfill three main requirements.[4] First is the capability to interface at least one qubit efficiently with optical photons (at telecommunication wavelengths for fiber-based systems) to establish remote entanglement at high rates. Second is the ability to store quantum states during entanglement generation; in particular, this requires qubit coherence times under full network activity to be longer than the time it takes to generate entanglement between nodes. Third is the capability to store several entangled states per node with a capability for high-fidelity operations between them to enable multi-qubit protocols such as error correction.

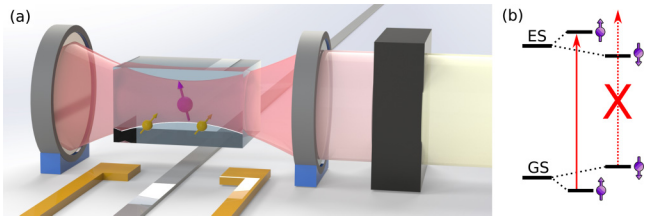

FIG. 2. Overview of a quantum network node based on color centers in diamond and simplified optical level scheme. (a) Schematic of a quantum network node in diamond, consisting of an optically active (communication) qubit (purple) embedded between two highly reflective mirrors (an optical cavity) to enhance the interaction strength of photons with the qubit. The state of the color center qubit can be swapped onto long-lived nuclear spin (memory) qubits in the surroundings (orange) using high-fidelity gates that employ microwave or RF pulses delivered via dedicated lines (gray). Tuning of network nodes to an optimal frequency operation point is, e.g., enabled by applying a static electric field via electrodes (yellow). Frequency conversion (black box) can be used to down-convert photons entangled with the state of the communication qubit to telecommunication wavelengths, for which photon transmission losses are low. The color center features spin-resolved optical transitions between an optical ground (GS) and excited state (ES), enabling optically mediated remote entanglement generation (b).

Color centers in diamond satisfy most of these requirements and have enabled some of the most advanced experimental demonstrations of quantum network protocols to date. We here give a concise, high-level overview of the achieved and projected key capabilities of color centers in diamond [see Fig. 2(a)], motivating a detailed treatment (and also including the relevant literature) in the remains of this article:

1. The color center contains an individually controllable, optically active spin (communication qubit), with access to several long-lived nuclear spins (memory qubits) in its surrounding. These memory qubits can be manipulated with high fidelity to free up the communication qubit and enable multi-qubit protocols. They have a long coherence time enabling robust state storage during subsequent network activity.
2. The internal level structure is suited to generate remote entanglement. In particular, color centers feature spin-state-selective optical transitions that can entangle the color center's spin-state with a photonic state, e.g., in the number/polarization/time basis [see Fig. 2(b)].
3. Optical emission of color centers is bright and can be collected with high efficiency, enabling high entanglement generation rates. This emission is in the visible to near-IR spectrum and thus at wavelengths that are associated with higher fiber transmission losses than for photons in the telecom band. However, it is possible to efficiently convert this emission to the telecom band while maintaining quantum correlations.
4. Diamond is a solid-state material, potentially enabling nanophotonic device fabrication at a large scale. Such devices can also be integrated with photonic circuits, and efficient interfacing of color centers embedded in such systems has been demonstrated.

IV. STATE OF THE ART OF DIAMOND-BASED QUANTUM NETWORKS

Two recent experiments showcasing the potential of color centers in diamond as quantum network node candidates can be seen in Fig. 3, together defining the state of the art in quantum networks. Figure 3(a) shows a laboratory-scale quantum network based on nitrogen-vacancy (NV) centers in diamond.[39] Three NV centers in separate cryostats, linked via optical fiber channels in a line configuration, are operated as independent quantum network nodes. The centers are set to a common optical emission frequency via electric field tuning (DC Stark shift).[19] The network is used to demonstrate the distribution of three-partite Greenberger–Horne–Zeilinger (GHZ) entangled states across the nodes, as well as entanglement swapping to achieve any-to-any connectivity in the network.[39] This network sets the state of the art for entanglement-based quantum networks.

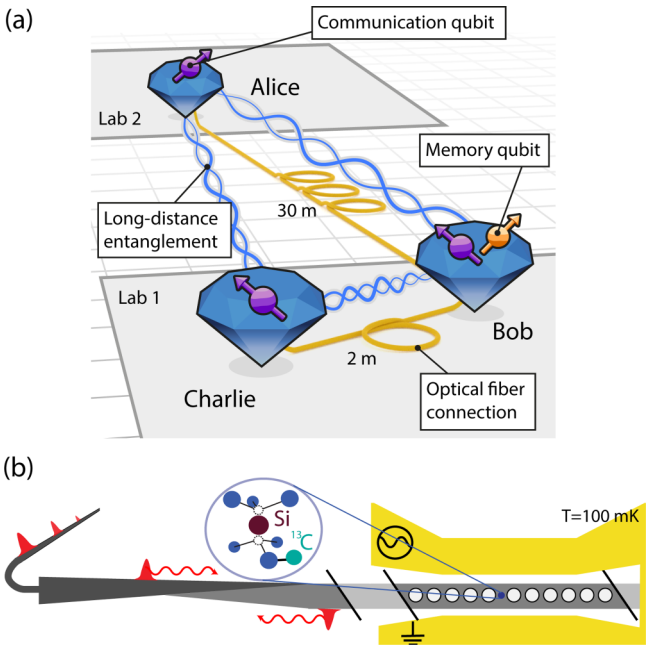

FIG. 3. State-of-the-art experiments showing the potential of color centers in diamond as quantum network nodes. (a) Schematic of a three-node quantum network based on nitrogen-vacancy (NV) centers in diamond, linked with optical fibers. One of the network nodes features a ^{13}C nuclear spin that is used as a memory qubit to store (part of) an entangled state and free up the communication qubit, while subsequent entanglement is created using this communication qubit a second time. Reprinted with permission from Pompili *et al.*, Science **372**, 259–264 (2021). Copyright 2021 AAAS.[39] (b) Schematic of a silicon-vacancy (SiV) center (blue circle) embedded in a fiber-coupled (dark gray) all-diamond photonic crystal cavity (light gray area with holes). Coherent emitter-cavity cooperativities $\sim$ 100 have enabled high-fidelity reflection-based spin–photon entanglement generation,[23] and control of individual ^{13}C nuclear spins via microwave pulses applied to the electron spin of the silicon vacancy spin qubit (yellow electrodes) has been demonstrated. Adapted with permission from Nguyen *et al.*, Phys. Rev. Lett. **123**, 1–6 (2019). Copyright 2019 The American Physical Society.[50]

Entanglement between the nodes is generated using a photon-emission-based scheme, in which spin–photon entanglement is locally generated at each NV node using microwave and laser pulses. The photonic modes are then interfered on a beam splitter, thereby erasing the which-path information. Subsequent photon detection heralds the generation of a spin–spin entangled state between two NV nodes.[19,45] Early experiments[19] had employed two-photon entangling schemes reaching fidelities $\sim 90\%$[20] at $\sim$ mHz rates. More recent experiments (including the three-node network discussed here) used a single-photon scheme[45] yielding fidelities $\sim 82\%$ at rates of ~ 10 Hz.[39] While the entanglement rate for the single click protocol only scales linearly with photon loss, the generated entangled state depends on the total phase difference of the laser excitation pulses and photon transmission paths, thus requiring phase stabilization throughout the experiment.[39,45] Additionally, this scheme intrinsically trades off entanglement fidelity with generation rate, as there is a possibility that both color centers emit a photon but one is lost. For the two-photon scheme, on the other hand, the color center's spin-state is flipped in between two excitation pulses, thus only requiring phase stability on the timescale between subsequent excitations and overcoming the fidelity-rate tradeoff. However, the quadratic scaling of the entanglement rate with photon losses for this scheme has prevented its use in multi-node entanglement experiments to date.

Importantly, these schemes generate entanglement in a heralded fashion, making the fidelity robust to photon loss and the generated entangled states available for further use. In the vicinity of the NV center, a ^{13}C nuclear spin is used as a memory qubit at the middle node, coupled to the NV center electron spin via the hyperfine interaction. The nuclear spin is controlled via tailored microwave pulses applied to the NV center spin[46] that simultaneously decouple the NV electron spin from the other nuclear spins. Characterization of the nuclear spin environment of an NV center has enabled communication qubit coherence times above 1 s.[47] In addition, entangled states have been stored in ^{13}C memory qubits for up to ~ 500 subsequent entanglement generation attempts.[39,48,49] Combined with the demonstrated capability of entanglement distillation (generating one higher fidelity state from two lower fidelity states)[38] and deterministic entanglement delivery (by generating entanglement between two nodes faster than it is lost, albeit not under full network activity),[45] these experiments highlight the potential of the NV center as a quantum network node. As we discuss in detail below, a main challenge for the NV center is the low fraction of emitted and detected coherent photons, limiting the entanglement rates.

Recently, a new class of defect centers in diamond has also gathered the attention of the community: the family of group-IV color centers in diamond, of which the negatively charged silicon-vacancy (SiV) center is the most studied member. Figure 3(b) shows a schematic of a SiV center embedded in a photonic crystal cavity, which increases the interaction of light with the communication qubit as compared to emission in a bulk diamond material (discussed in Sec. VII below). Spin–photon entanglement with fidelity $\geq 94\%$ has been generated in this system using cavity quantum electrodynamics (cQED) reflection-based schemes, in which photons impinging on the cavity containing the communication qubit are reflected or transmitted depending on the spin-state of the communication qubit.[50] While entanglement between distant SiV centers has not yet been demonstrated, strong collective interactions between two SiV centers[51] in the same cavity and probabilistic entanglement generation between two SiVs[52,53] in one waveguide have been observed. In addition, photon outcoupling efficiencies from the emitter-cavity system into fiber >0.9 have enabled the demonstration of memory-enhanced quantum communication.[23] This experiment sets the state of the art for quantum repeater experiments.

Additionally, recent experiments have demonstrated key quantum network node capabilities, including dynamical decoupling of the SiV spin from the bath with coherence times above 1 ms,[22,54] ^{13}C nuclear spin initialization, control, and readout via the central SiV electron spin,[55,56] and frequency control of SiV centers via strain tuning.[53,57,58] Combined with recent efforts to fabricate SiV centers in nanophotonic waveguides at a large scale and their integration in photonic circuits,[58] these results show the potential of silicon-vacancy centers and other closely related group-IV color centers as nodes for a quantum network (see Sec. VII).

V. OPTICAL AND SPIN PROPERTIES OF COLOR CENTERS IN DIAMOND

Nitrogen-vacancy and group-IV color centers in diamond feature different structural symmetries, which result in different properties of their spin–photon interface. Here, we briefly introduce the most important differences between those color centers in diamond, to the point necessary to understand current limitations and research directions described in the remains of this article; we refer the reader to the many excellent articles that cover the physics of these color centers in great detail.[78,83,84] In this article, we consider all color centers to be in the negative charge state, except where indicated differently; this negative charge state is the one most commonly studied and used in experiments geared toward entanglement generation. We also note that while other recently investigated color centers in diamond, such as Mg-related defects,[85] show some initial promise for quantum applications, we do not discuss them here due to their early phase of study.

Figure 4 shows the difference in atomic structure of nitrogen-vacancy (NV) centers and group-IV color centers [consisting of silicon-vacancy (SiV),[56,64,65] germanium-vacancy (GeV),[69] tin-vacancy (SnV),[24,70] and lead-vacancy (PbV)[74] centers]. An NV center is formed by a nitrogen atom replacing a carbon atom of the diamond lattice, next to a lattice vacancy, giving rise to a C_{3v} symmetry [Fig. 4(a)]. The NV center possesses a permanent electric dipole moment, making the optical transition frequencies sensitive to charge fluctuations in its environment.[78] This sensitivity to electric fields has been used as a resource to tune different NV centers onto resonance,[86] counteracting local strain inhomogeneities in the host diamond crystal, which shift the transition frequencies of color centers. However, it has also hindered the nanophotonic integration of NV centers due to the degradation of their optical properties near surfaces.[87,88]

The NV center features an outstanding spin energy relaxation time of over 8 h.[89] Quantum states have been stored in the NV center's electronic spin for over 1 s by decoupling the electron from unwanted interactions in its environment using

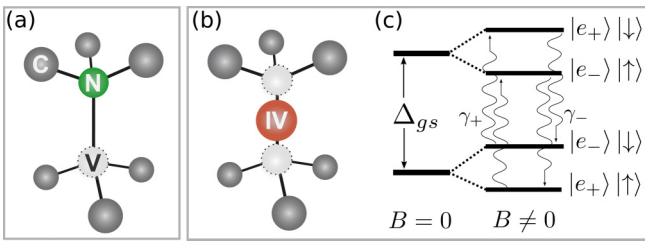

FIG. 4. Schematic atomic structure of NV (a) and group-IV (b) color centers in diamond and ground state level structure of group-IV color centers (c). The inversion symmetry of group-IV color centers leads to a vanishing permanent electric dipole moment, making those defect centers suitable for integration in nanophotonic structures. This structure also results in orbital and spin double degeneracies in the ground and excited state (c, only ground state shown for simplicity) that are lifted by (mostly) spin–orbit coupling (Δ_{gs}) and by application of an external magnetic field (B), respectively. Phonon-induced transitions (γ_+/γ_-) between orbital states limit (communication) qubit coherence times (see text).

tailored microwave pulse sequences.[47] Fidelities in quantum networks experiments have reached $> 0.99\%$ for single qubit gates and $\sim 98\%$ for two-qubit gates (between NV electron and ^{13}C nuclear spins).[39]

For group-IV color centers, the group-IV atom takes an interstitial lattice site between two lattice vacancies. The resulting inversion-symmetric D_{3_d} structure of the defect [Fig. 4(b)] results in no permanent electric dipole and thus a first-order insensitivity to electric field fluctuations. As a consequence, tuning optical transition frequencies of group-IV color centers by electric fields is relatively inefficient,[90,91] potentially necessitating other techniques (discussed in Sec. VII). On the other hand, the vanishing permanent electric dipole makes these color centers excellent candidates for integration into photonic nanostructures (also discussed in Sec. VII).

Group-IV emitters also feature a different level structure than the NV center: both optical ground and excited states are formed by doubly degenerate orbital states, which are each split into pairs by spin–orbit interaction and the Jahn–Teller effect. Under an external magnetic field, the double spin degeneracy in each pair ($S = 1/2$) is lifted.[64,83,92] The qubit subspace can then, for example, be defined over the two opposing spin sublevels of the optical ground state's lower orbital branch [see Fig. 4(c)]. This, however, means that direct microwave driving of the qubit levels is forbidden in first order, as one would need to flip both spin and orbital quantum numbers. Typically, this complication is overcome by working with emitters with transversal strain $\sim \Delta_{gs}$, which mixes the orbital levels, such that the qubit state can be effectively described by the spin only and thus be driven with higher efficiency.[56] Coherent microwave control of group-IV color centers has recently been demonstrated for SiV centers,[54,56] with infidelities on the percent level.[54] For other group-IV color centers, only incoherent microwave driving of spin transitions has been achieved so far.[24,69] The reported infidelities for coherent SiV control are a result of qubit dephasing during microwave pulses, as relatively low Rabi frequencies (~ 10 MHz) are used to limit heating-induced decoherence. It is expected that the use of superconducting waveguides[93] will further improve microwave pulse fidelities (as a result of potentially significantly reduced ohmic heating) for all color centers.

Spin dephasing in the group-IV qubit subspace is dominated by phonon-assisted transitions to the upper ground state orbital branch, which leads to the acquisition of a random phase: while the phonon transitions are in principle spin-conserving, the detuning between the spin states varies depending on which orbital state is occupied [see Fig. 4(c)].[94,95] In Table I, we map reported ground state splittings into a concrete performance metric by extrapolating the temperatures T_{oper} below which we expect an orbital coherence time > 100 ms due to low phonon occupation. From this, we see that a larger ground state splitting (associated with stronger spin–orbit coupling strengths for heavier ions) is beneficial for maintaining long qubit coherence. However, this requires higher microwave driving powers for similar off-axis strain values, as the strain-induced orbital mixing is related to the spin–orbit coupling strength and thus the overlap between orbital states is reduced.[56] All-optical spin control schemes represent an alternative to microwave driving, as demonstrated, e.g., for SiV[63,96,97] and GeV[69]

TABLE I. Overview of optical and orbital properties of group-IV (SiV, GeV, SnV, PbV) and NV defect centers in diamond. All listed numbers are approximate values. We consider all defects to be in the negative charge state. The Debye–Waller factor characterizes the fraction of radiative emission into the ZPL, while we define the quantum efficiency as the ratio of radiative to all decay. Ground state splitting denotes splitting between orbital states in the optical ground state of group-IV color centers [see Fig. 4(c) and text]. T_{oper} is the calculated operation temperature below which the expected orbital lifetime is above 100 ms. We estimate this temperature by calculating the phonon transition rate $\gamma_+ \propto \Delta_{gs}^3/(e^{(\Delta_{gs}/k_B T)} - 1)$ [see Fig. 4(c)], where Δ_{gs} is the orbital ground state splitting, T is the temperature, and k_B is the Boltzmann constant (as $\gamma_- > \gamma_+$, γ_+ determines the qubit coherence times), as in Refs. 24 and 70. We then find the proportionality factor to map this to a concrete temperature by using the measured values of Ref. 65. We note that there are currently different findings about the exact parameters for the lead-vacancy center in diamond. We, therefore, include two pairs of values with their respective references.

Vacancy	ZPL wavelength (nm)	Quantum efficiency (%)	Debye–Waller factor	Radiative lifetime (ns)	Ground state splitting (GHz)	T_{oper} (K)
SiV	737[23]	(1–10)[52,59]/60[60]	(0.65–0.9)[61,62]	1.7[52,63]	50[63–65]	0.1
GeV	602[66]	(12–25)[67,68]	∼0.6[69]	(1.4–6)[21,66]	170[69]	0.4
SnV	620[24,70]	∼80[70]	0.57[71]	(4.5–7)[24,72,73]	850[24,70]	1.8
PbV	520[74]/555[75–77]	Not known	Not known	>3[74]/3.5[75–77]	5700[74]/3900[77]	9.8/7.0
NV	637[78]	>85[79]	0.03[80,81]	(11–13)[49,80,82]	Not applicable	Not applicable

centers. For SnV centers, spin initialization by optical pumping has been observed.[24] Another way of defining and driving a qubit could be to mix the (mostly) orthogonal spin components via an off-axis magnetic field and use surface acoustic waves to drive phonon transitions between the orbital levels, with demonstrated Rabi frequencies ~ 30 MHz.[98] Such an off-axis magnetic field, however, is at odds with achieving the high spin cyclicity needed for single shot spin-state readout and high-fidelity entanglement generation, necessitating a careful tradeoff.[56] For magnetic fields aligned with the color center's symmetry axis, readout fidelities above 99.99% have been achieved.[50,54]

Table I also shows a comparison of the most important optical properties for both group-IV color centers and nitrogen-vacancy centers in diamond. To generate entanglement, only the fraction of coherent photons emitted in the zero-phonon line (ZPL, for which no lattice vibrations assist the transition[78]) can be used.[19] Importantly, all quantified zero-phonon-line emission fractions for group-IV color centers are significantly larger than for the NV center, as the inversion symmetry of these emitters causes their excited states to have greater overlap with the optical ground state,[92] resulting in a higher fraction of direct photon transitions.[99,100] While most recent quantum memory experiments with SiV centers have operated in dilution refrigerators (see below) in order to suppress the thermal phonon population,[54,97] the SnV center with relatively high expected operating temperature requirements might be particularly promising for use as a quantum network node. We note that the neutral charge state variants of group-IV color centers are also promising, as they potentially combine the favorable spin–photon interface of negative group-IV color centers with the excellent spin coherence times and easy qubit manipulation of negative nitrogen-vacancy centers.[92,101–104] We do not discuss it extensively here due to its early stage of the study.

VI. ENHANCING THE MEMORY QUBITS

We now discuss the state of the art and future research directions regarding the memory qubits of color centers in diamond. The most common isotope of carbon is ^{12}C. However, the ^{13}C isotope with natural abundance of about 1.1% carries a nuclear spin of 1/2. In the last decade, techniques have been developed (mostly on NV-based systems) to control these nuclear spins via the position-dependent hyperfine coupling. Universal nuclear spin control using electron decoupling sequences that are in resonance with a single ^{13}C spin has been demonstrated.[46] This has enabled the demonstration of coherence times above 10 s, and electron-nuclear gate fidelities $\sim 98\%$ for individual ^{13}C spins in NV-based systems.[38,105] Additionally, up to one memory qubit per communication node has been used in an NV-based quantum network setting to date.[38,39] For the case of SiV centers (and group-IV color centers in general), on the other hand, the spin-half nature of the system leads to a vanishing first-order sensitivity of decoupling sequences to individual ^{13}C hyperfine parameters, thus requiring long decoupling times (and/or potentially off-axis magnetic fields that are at odds with a high spin cyclicity of optical transitions) to isolate out single nuclear spins. So far, electron-nuclear gate fidelities have been limited to $\sim 59\%$ for SiV centers;[50] ^{13}C nuclear spins close to group-IV color centers have not yet been used in quantum networks experiments.

The first area of research is thus to extend the number of available nuclear spin qubits per network node, as well as their control speeds and fidelities. Recently developed gate schemes based on interleaving radio frequency (RF) driving of ^{13}C nuclear spins (to control previously unaddressable qubits) with dynamical decoupling pulses (to decouple from the spin bath) have allowed the creation of a local quantum register of an NV communication qubit and up to nine surrounding nuclear spin qubits [see Fig. 5(top)] that allow entangled state generation between all pairs of qubits [Fig. 5(bottom)], creation of a local seven-qubit GHZ state as well as memory coherence times of single and two-qubit states of over 10 s.[105] This result (achieved on a similar device as used for distant entanglement generation[19,38,39]) shows that it is realistic to expect diamond-based quantum nodes containing many qubits in the near-term future. Such registers could enable scalable, modular quantum computation,[40] and universal, fault-tolerant error correction.[46,106–108] Additionally, we expect that RF driving of nuclear spins will overcome current limitations in manipulating nuclear spins for group-IV color centers, as the nuclear spin transition frequencies depend on the hyperfine parameters on the first order in this case.[56] Overcoming issues related to sample

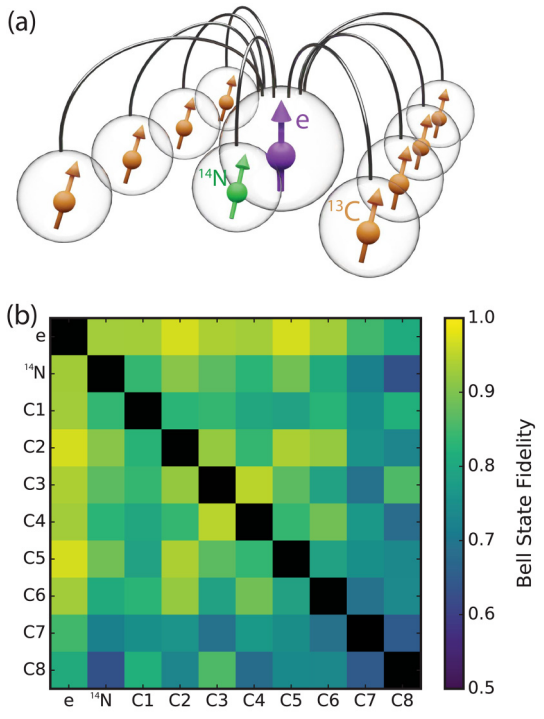

FIG. 5. State-of-the-art research for increasing memory qubit numbers and control for color centers in diamond. (a) Schematic overview of a local ten-qubit quantum register in diamond, formed from a nitrogen-vacancy center (purple), a native ^{14}N nuclear spin, and eight surrounding ^{13}C nuclear spins. (b) Connection map of the spin register in (a), demonstrating entanglement generation between all pairs of qubits in the register. Adapted with permission from Bradley *et al.*, Phys. Rev. X **9**, 31045 (2019). Copyright 2019 Author(s), licensed under creativecommons.org/licenses/by/4.0/legalcode.[105]

heating and background amplifier noise could then also enable to address multiple nuclear spins simultaneously, thus reducing decoherence associated with long gate times.[105] Additionally, crosstalk between nuclear spins as well as unwanted coupling to other spins could be reduced when using the full information of the environment of a color center[109] (potentially acquired while involving automated techniques[110]) to simulate and tailor gate sequences for a specific spin environment, and computationally optimizing them for overall protocol fidelity. Another way of extending the number of controllable nuclear spin qubits per node is to also employ the nuclear spin of a nuclear spin containing color center atom isotope, e.g., of ^{14}N (nuclear spin of 1)[111] or ^{29}Si (nuclear spin of 1/2).[65] While the electron-nuclear gate times for these intrinsic nuclear spins can be relatively fast thanks to the strong (∼MHz), always-on hyperfine coupling to the color center's electron spin, they are for the same reason more susceptible to dephasing from uncontrolled electron dynamics during entanglement generation (see paragraph below). Thus, despite slower gate times, more weakly coupled 13C spins (∼kHz) are commonly used in experiments that require high fidelity storage of a quantum state during subsequent entanglement generation attempts.[38,39] In general, the choice of memory qubit depends on the requirements of a specific application.

A second research direction is to increase the coherence time per available memory qubit under full network activity (in particular, entanglement generation). The "always-on" nature of the hyperfine interaction of ^{13}C nuclear spin memory qubits and the NV center has limited memory coherence in quantum networks to ∼500 entanglement generation attempts.[39,49] Uncontrolled electron dynamics, which result for instance from control infidelities and stochastic electron spin initialization during an entangling sequence, cause dephasing of the nuclear spin memory qubits.[49] Techniques such as higher magnetic fields at the color center location can speed up gate times and shorten the entanglement generation element, thus reducing the time over which random phases can be picked up.[39,49] Additionally, decoupling pulses on the memory qubits that suppress quasi-static noise in the environment have shown initial promise to prolong nuclear memory qubit coherence under network activity for NV centers.[49] Other promising routes to extend the nuclear spin memory coherence time involve reducing the color center's state-dependent coupling strength (the main dephasing channel), e.g., by employing decoherence-protected subspaces (formed from two or more individual spins, or pairs of strongly coupled spins that mostly cancel the state-dependent hyperfine interaction term),[47,48,112] and using isotopically purified samples for which weakly coupled ^{13}C nuclear spin qubits can be controlled[113,114]). Other methods are to engineer systems of coupled defects (e.g., involving a ^{13}C nuclear spin qubit coupled to a P1 center in the vicinity of an NV center[115] or to use the nitrogen nuclear spin of a second NV center (whose nitrogen nuclear spin is used as a memory) in proximity to the communicator NV center.[116,117]

VII. ENHANCING THE SPIN–PHOTON INTERFACE

Optically mediated entanglement generation with high rates requires quantum network nodes with efficient spin–photon interfaces. However, the relatively high refractive index of diamond (∼ 2.4) leads to significant total internal reflection at the diamond–air interface, which limits photon collection efficiencies. Entanglement rates are further reduced by the finite fraction of photons emitted into the zero-phonon line (ZPL) that can be used for entanglement generation (see Sec. V above). Thus, techniques that can increase the fraction of collected photons at ZPL wavelengths, and/or increase the interaction of light with the emitter are required. Here, we discuss both strategies as well as their suitability for enhancing the spin–photon interface of different diamond color centers, and the state of the art and future avenues for this research. We note that strong light–matter interactions also open the door to entangling schemes alternative from the photon-emission-based protocols discussed above,[7,8] e.g., based on spin-dependent cavity reflections.[9,23,118–120]

A. Strategies for enhancing the spin–photon interface

The two most common strategies to enhance the spin–photon interface are by increasing the photon flux at the detector through improvements in photon collection, and through cavity or Purcell enhancement, which increases light–matter interaction and spontaneous emission rates (see Fig. 6). Here, we only give a brief

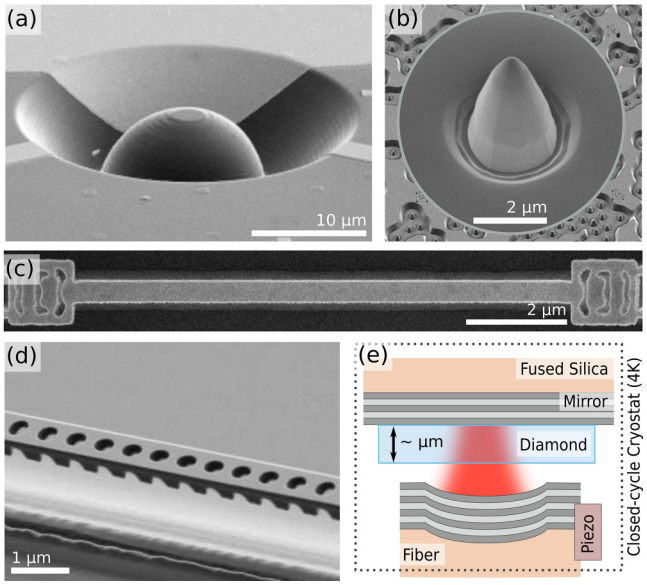

FIG. 6. Devices used to enhance the spin–photon interface of color centers in diamond. Solid immersion lenses[126] (a), parabolic reflectors [(b), adapted with permission from Wan *et al.*, Nano Lett. **18**, 2787–2793 (2018). Copyright 2017 American Chemical Society[130]], and waveguide [(c), SEM image of the device from the same chip used in Ref. 143] allow us to enhance photon collection efficiencies from embedded color centers, compared to emission in a bulk host material. Photonic crystal[146] [(d), adapted with permission from Burek *et al.*, Optica **3**, 1404 (2016). Copyright 2016 The Optical Society (OSA)[147]] and open, tunable micro-cavities [(e), adapted with permission from Ruf *et al.*, Phys. Rev. Appl. **15**, 024049 (2021). Copyright 2021 Author(s), licensed under creativecommons.org/licenses/by/4.0/legalcode[82]] enhance the collection efficiency while modifying the nanophotonic environment at the same time. This allows to additionally enhance the number of photons emitted at a certain wavelength via the Purcell effect, compared to collection enhancement tools.

overview of these methods and refer to the many extensive diamond-color-center specific review articles that cover them in detail (see, e.g., Refs. 84 and 121–123).

1. Collection efficiency enhancement

A common method to enhance collection efficiency from color centers in diamond is to fabricate dome-shaped solid immersion lenses around the emitters [Fig. 6(a)], which leads to a higher fraction of light being collected, as total internal reflection is avoided by the light striking the diamond surface at a perpendicular angle. These devices have been used to increase emission from NV,[124–128] SiV,[63,64] and GeV[69,129] centers; all diamond-based remote entanglement generation experiments reported to date have used these devices, with detection efficiencies of emitted photons of up to $\sim 10\%$.[126]

A second class of collection efficiency enhancement methods is based on nanostructures that modify the far-field emission of a dipole emitter. These structures comprise different dimensions, designs, and supported wavelength ranges and include parabolic reflectors[130,131] [Fig. 6(b)], nanopillars,[132] nanowires,[133,134] nanocones,[135] gratings[136,137] and diamond waveguides[21,52,58,138–143] [Fig. 6(c)]. While they offer large-scale fabrication and higher collection efficiencies than solid immersion lenses (reported dipole-waveguide coupling efficiencies above 55%[58,131]), the demands in nano-fabrication and color center placement are more stringent than for solid immersion lenses, and emitters have to be brought in close proximity to nano-fabricated surfaces. This proximity to surfaces is believed to be the cause of optical instability for some diamond color centers, as discussed in detail below. Such instabilities make it challenging to produce indistinguishable photons from remote centers as required for entanglement generation.[144,145]

2. Purcell enhancement

Another way of enhancing the spin–photon interface is to embed the dipole emitter inside an optical cavity, making use of the Purcell effect, described by the Purcell factor F_P. This factor scales with the ratio of the cavity quality factor, Q (inversely proportional to the cavity's energy decay rate), to the cavity mode volume, V (describing the cavity light field confinement).[119] Briefly, a cavity enhances the density of states around its resonance frequency such that the spontaneous emission of an embedded dipole emitter is increased when on resonance with the cavity, following Fermi's golden rule. Additionally, the cavity funnels emitted light into a well-defined mode that can be readily matched, e.g., to that of optical fibers. A commonly used parameter to quantify the radiative emission enhancement by the cavity (defined as the ratio of the dipole–cavity emission, γ_{cav}, compared to the emission in a homogeneous medium, $\gamma_{hom} = \gamma_{rad} + \gamma_{nonrad}$) is the cooperativity, C, defined as

$$C = \frac{4g^2}{\kappa\gamma_{hom}} = \frac{\gamma_{cav}}{\gamma_{hom}} = F_P\beta_0\eta, \tag{1}$$

where g is the dipole–cavity coupling rate, κ is the energy decay rate from the cavity, γ_{rad} is the free-space radiative emitter decay rate, γ_{nonrad} is the non-radiative emitter decay rate, β_0 is the fraction of photon emission from the emitter into the zero-phonon line (given by the Debye–Waller factor), and η is the quantum efficiency (defined as the ratio of radiative to all decay). While this quantifies the efficiency of the spin–photon interface, it does not take into account the coherence of the emitter: in practice, solid-state emitters often experience dephasing due to unwanted interactions with the environment of the solid-state host, characterized by a pure dephasing rate γ_{dep}, which manifests in broadening of the optical transitions above the lifetime-limited value.[50,81,143,148–150] Therefore, it is useful to introduce the coherent cooperativity, C_{coh}, which quantifies the ratio of coherent decay into the cavity mode to undesired decay, and is given as[123,151]

$$C_{coh} = \frac{4g^2}{\kappa(\gamma_{hom} + \gamma_{dep})} = C\frac{\gamma_{hom}}{\gamma_{hom} + \gamma_{dep}}. \tag{2}$$

C_{coh} can be interpreted as the probability of coherent atom–photon interaction and plays an important role in the fidelity and efficiency of many near-deterministic quantum protocols (which require $C_{coh} \gg 1$).[151]

To date, cavity enhancement of diamond color centers has been demonstrated for different implementations, including diamond-on-insulator whispering gallery mode resonators[80,152] and nanodiamond plasmonic antennas.[153] Another class of devices is based on the coupling of non-diamond resonators to color centers in nanodiamonds[154–157] or diamond films.[158–160] Open and tunable micro-cavities geometries have also been demonstrated for embedded nanodiamonds[161–166] and thin diamond membranes[67,81,82,167,168] [Fig. 6(d)]. Steady progress in diamond nanofabrication has also led to all-diamond photonic crystal cavities[23,50–52,56,87,169–173] [Fig. 6(e)], with demonstrated coherent cooperativities exceeding 100 for the case of the SiV center.[23]

Quantum network applications also require the efficient coupling of light from these nanostructures to optical fibers. Different methods of coupling to fiber-based communication channels have been realized to date, including optimized free-space couplers with efficiencies up to $\sim 25\%$,[143,174] notch couplers with efficiencies $\sim 1\%$,[52] grating couplers with efficiencies $\sim 30\%$,[152,175] and double-[142,176,177] and single-[23,51,56,178] sided fiber-tapers with efficiencies of up to $\sim 90\%$.

B. Looking forward: Key challenges and potential solutions

Having introduced different theoretical concepts to increase the spin–photon interface of color centers in diamond, we now discuss the experimental state of the art of such enhancement, highlighting key challenges and potential research directions.

1. NV centers

While the nitrogen-vacancy (NV) center has been a workhorse of quantum network demonstrations with color centers in diamond, its low fraction of optical emission at the zero-phonon line (ZPL) frequency of 3%, as well as limited collection efficiency from solid immersion lenses currently restrict local entanglement generation rates to < 100 Hz.[39,45] Due to their permanent electric

dipole moment, NV centers experience large spectral shifts on short timescales caused by charge fluctuations in the environment when close to surfaces (∼micrometers).[88] As a result, despite reported Purcell factors of up to 70 in small mode-volume photonic crystal cavities,[87] the regime of $C_{coh} \geq 1$ has remained out of reach. We note that the origins of the surface noise are still a subject of active research and that recent experiments geared at understanding the effect and origins of surface noise on the NV center spin,[179] and the local electrostatic environment of NV centers[180] show promise toward understanding the causes of surface charge noise. Combined with proposals for active optical driving to reduce spectral diffusion effects,[181] this could revive the field of NV centers in nanophotonic structures in the future.

The challenge imposed by nearby surfaces can be circumvented by embedding μm-thin diamond membranes between two highly reflective mirrors.[182] A recently reported fabrication technique has formed NV centers with bulk-like optical properties in μm-thin diamond membranes that can be embedded in such cavities via a combination of electron irradiation, high temperature annealing, and a tailored diamond etching sequence[88] [Fig. 7(a)]. This has allowed for the first demonstration of resonant excitation and detection of optically coherent NV centers, Purcell enhanced by an optical cavity,[82] as would be required for cavity-enhanced entanglement generation. However, the Purcell enhancement in this experiment was limited to ∼3, (mostly) due to cavity-length fluctuations ∼100 pm induced by a closed-cycle cryocooler. Previously, it has been shown (using off-resonant excitation) that Purcell enhancement factors of up to 30 (corresponding to 46% of light emitted in the ZPL) can be achieved for such open microcavities in a liquid helium bath cryostat (featuring lower cavity-length fluctuations)[81] [Fig. 7(b)]. Combined, these experiments demonstrate that there is a near-term path from the current $C_{coh} \sim 0.1$ toward $C_{coh} \sim 1$ and coherent photon collection efficiencies ∼10%. In addition, recent results suggest that it should be possible to reach the required pm-scale cavity-length fluctuations even in closed-cycle cryostats,[32,183] which would remove the need for a liquid helium infrastructure at each quantum network node.

Another active area of research is to create shallow, stable NV centers[184–186] at controlled locations; both the electron irradiation technique employed in Ref. 82 as well as recently introduced laser-writing techniques[187] can form optically coherent NV centers but rely on native nitrogen in the sample to recombine with introduced lattice vacancies and thus miss precise control of the site of NV center formation. However, for maximal Purcell enhancement, NV

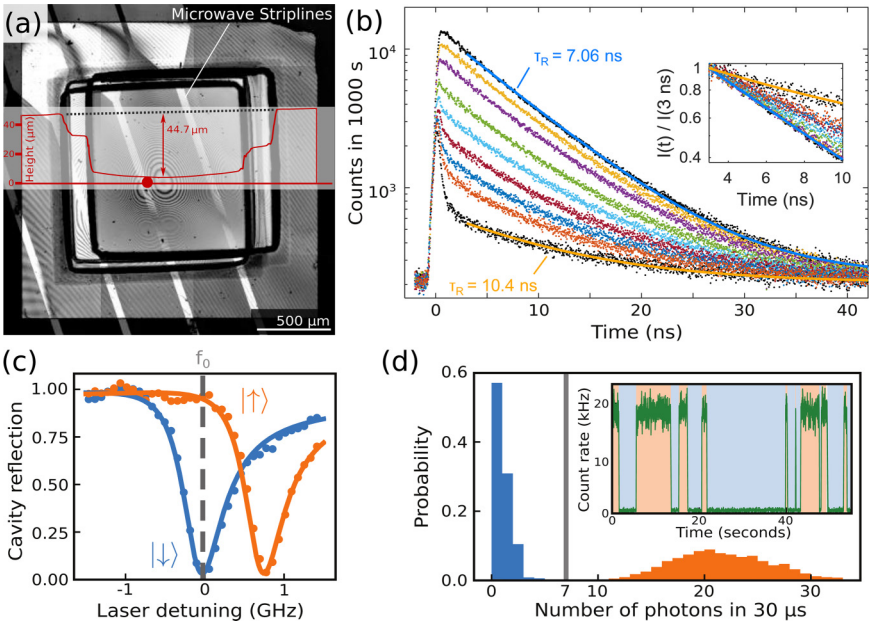

FIG. 7. State-of-the-art research for enhancing the spin–photon interface of color centers in diamond for quantum networks applications. (a) Confocal microscope image of a typical μm-thin etched diamond sample containing NV centers with bulk-like optical properties, bonded via van der Waals forces to a mirror containing microwave strip lines. The location and direction of a sample height trace measurement is indicated with a red arrow. Such samples have recently enabled the first demonstration of resonant excitation and detection of coherent Purcell enhanced NV centers.[82] Adapted with permission from Ruf *et al.*, Nano Lett. **19**, 3987–3992 (2019). Copyright 2019 American Chemical Society.[88] Further permissions related to the material excerpted should be directed to the American Chemical Society. (b) NV center excited state decay in the ZPL for different emitter-cavity detunings for an NV center in an open micro-cavity under pulsed off-resonant excitation. Inset shows normalized decay curves. Adapted with permission from Riedel *et al.*, Phys. Rev. X **7**, 1–8 (2017). Copyright 2017 Author(s), licensed under creativecommons.org/licenses/by/4.0/legalcode.[81] (c) Spin-state-dependent reflection spectrum of a SiV center in a critically coupled photonic crystal cavity with $C_{coh} \sim 100$. The spin-state dependent photon reflection with high collection efficiency enables spin-state readout with fidelity $> 99.9\%$ in a single shot (d) and has recently enabled the first demonstration of memory-enhanced quantum communication. Figures (c) and (d) are adapted with permission from Bhaskar *et al.*, Nature **580**, 60–64 (2020). Copyright 2020 Springer Nature.[23]

centers should be positioned at an antinode of the cavity field. While such a precision can be achieved using ion implantation, recent research has shown that NV centers created via this technique suffer from increased optical linewidths compared with NV centers formed during growth,[188] even after extended high temperature treatments to restore the diamond lattice.[189]

While it will remain challenging to achieve coherent cooperativities $\gg 1$ (and thereby enter the near-deterministic spin–photon interface regime[151]), the open cavity approach is projected to speed up current emission-based entanglement generation schemes by $\sim$2 orders of magnitude.[82] This could allow for continuous deterministic entanglement generation (generating high-fidelity entanglement faster than it is lost) and enable experiments such as the formation of a quantum repeater surpassing direct transmission,[190] and device-independent quantum key distribution[191] using NV centers.

2. Group-IV color centers

The first-order electric field insensitivity of group-IV color centers in diamond[24,66,72,74,92,143,192–194] has enabled the demonstration of close-to-lifetime-limited optical transitions even in heavily fabricated nanophotonic structures.[21,52,56,58,143,193] To date, photonic crystal cavity coupling of group-IV color centers in diamond at low temperatures has been demonstrated for SiV[23,50–52,56] and SnV centers,[73] with demonstrated $C_{coh} > 100$ for the case of the SiV center.[23] This system allows for spin-state dependent photon reflection, enabling high-fidelity single shot spin-state readout with demonstrated fidelities $> 99.9\%$ [see Figs. 7(c) and 7(d)]. This has recently enabled the first demonstration of memory-enhanced quantum communication.[23]

A key requirement for many remote entanglement generation schemes is the ability to tune two group-IV color centers located on separate chips to a common resonance frequency. So far, tuning the emission frequency of group-IV emitters has been demonstrated using strain,[53,57,58,95,195] electric fields,[90,91] and Raman-type[52,196] schemes (although the latter is only compatible with emission-based entanglement generation schemes) but only for a single emitter or several emitters in one structure. The first two tuning techniques deform the orbitals of the group-IV color centers, and thus the color center's inversion symmetry is broken, leading to an observed increase in transition linewidths and spectral diffusion under applied external strain/electric field (potentially due to an increase in sensitivity to charge noise in the environment). We note that recent experiments indicate a larger tuning range of transitions for strain tuning (as compared to electric field tuning) for the same induced line broadening.[58,90,91]

While close-to-lifetime-limited linewidths of group-IV color centers in nanophotonic structures have been observed, experiments still routinely show spectral shifts and charge instabilities, leading to broadening on the order of several lifetime-limited linewidths[51,56,58,143] as well as large local strain fields. While dynamic strain tuning can be used to suppress slow spectral diffusion (seconds timescale),[53] it is challenging to improve the homogeneous linewidth (sub-microsecond timescale) that enters the coherent cooperativity using this approach. Typically, emitters are created by high-energy implantation, followed by a high temperature annealing step to form group-IV vacancy centers and to reduce the effects of lattice damage from the implantation process.[70,71,77] However, there is evidence that even such high temperature treatments cannot fully recover the original diamond lattice.[188] A recently developed promising method to overcome this limitation employs low energy shallow ion implantation, combined with overgrowth of diamond material.[197] Another strategy could be to combine low-density ion implantation with electron irradiation, to reduce the amount of damage created in the lattice via the (heavy) ion implantation.[198] Combined with controlled engineering of the diamond Fermi level,[102,199–201] these techniques could increase the quality and stability of group-IV color center optical transitions.[51,56,58,72,74,143]

Another area of active development involves the design and fabrication of the nanophotonic structures. Despite recent progress,[202,203] growing high quality, thin film diamond on large scales is challenging, and (to the best of our knowledge) there is no wet processing technique that can etch bulk single-crystal diamond along its crystal planes, thus requiring either laborious thinning of diamond on a low index material or sophisticated techniques to produce suspended, wavelength-thick diamond devices. While initial research focused on creating sub-μm-thin diamond films via selectively wet-etching a localized graphitized diamond layer[204–209] or etching down a super-polished thin diamond membrane,[60,87,169,170,210] these methods typically feature low device yield (as a consequence of challenges in device handling and initial material thickness variations). Thus, recent research has focused on fabricating structures directly in commercially available bulk diamond material via a combination of a hard mask and an angled diamond etch (leading to a triangular device cross section),[52,56,138,146,211–213] or a quasi-isotropic (dry) undercut etch, which selectively etches along certain diamond crystal planes (leading to rectangular device cross section).[58,174,214–218] Known limitations to these processes include mixing of TE- and TM-like modes that will ultimately limit device quality factors for triangular devices as well as a relatively high bottom surface roughness for quasi-isotropic etched devices (although it is worthwhile to note that the fabrication parameter space is somewhat less explored for the latter technique).

Currently, all listed fabrication methods routinely achieve photonic crystal cavity quality factors $\sim 10^4$, about two orders of magnitude lower than simulated values.[216] These deviations are caused by a combination of surface roughness,[56] non-uniform hole sizes,[73] and deviations from the expected device cross section;[217] we expect that an order-of-magnitude improvement in device quality factors is within reach upon further optimization. Furthermore, although photonic crystal nanocavities can be designed and fabricated to resonate at the ZPL frequency, they are especially sensitive to process variations, leading to a resonance wavelength spread of ~ 5 nm across devices.[216] Nonetheless, this spread in frequency may be overcome by cavity tuning methods,[52,87,219] which are in any case needed for the precise overlapping of the ZPL and cavity frequency.

As nanofabrication methods are constantly refined, it is also likely that current methods of optimally aligning color centers within nanophotonic structures (to guarantee maximal overlap between the optical mode and the dipole emitter) can be further improved. Toward this end, various methods have already been

demonstrated, including the targeted fabrication around pre-located centers,[130] or ion implantation into devices using either masks[56] or focused implantation.[52,58] Compared to the SiV center for which $C_{coh} \sim 100$ has been demonstrated, GeV and SnV centers have intrinsically higher radiative efficiencies and thus potentially higher cooperativities, which may increase cavity-QED-based protocol fidelities (see discussion below).

We note that group-IV color centers in diamond are also suitable for integration into tunable, open micro-cavities, as recently demonstrated for GeV[67] and SiV[167,168] centers at room temperature. It should be possible to achieve $C_{coh} \gg 1$ for these systems, potentially providing a viable alternative to the more fabrication-intensive nanostructures.

VIII. TOWARD LARGE-SCALE QUANTUM NETWORKS

Having discussed the core quantum network components based on diamond color centers, we now turn to what is required to build these into a network capable of distributing entanglement over large distances at high rates.

First, a future quantum Internet will likely make use of existing fiber infrastructure. This necessitates matching the photon wavelength from the network node to the telecommunication bands using quantum frequency conversion. Recently, it has been demonstrated that spin–photon entanglement can be preserved after frequency downconversion of a ~ 637 nm photon entangled with the spin-state of the NV center to telecommunication wavelengths (~ 1588 nm).[222] Similar conversion techniques can be applied to other color centers and quantum systems.[223–227] Future work will focus on increasing the system efficiency and potentially integrating on-chip conversion (see below).

Second, it will be important to lower the footprint and cost of experimental setups. Since a large-scale quantum network will likely make use of already existing fiber connections, data centers are natural candidates for the placement of quantum repeater nodes. An important first step could thus be to shrink experimental setups to the standard 19-in. server racks used in industry[228] and ruggedize components so that the need for manual intervention can be kept to a minimum, and the systems can tolerate the conditions prevailing at such locations.

Third, future quantum networks covering large distances will require many quantum repeater stations—each with a large number of qubits—for multiplexing, purification, and error-correction. For example, 5–10 repeater stations with kilohertz entangled bit (ebit) rates need a total of $O(10^8)$ data qubits to reach mega-ebits per second communication.[229] Although color center devices are already produced using standard nanofabrication techniques, the needed scale for high-rate, high-fidelity networks would require large-scale manufacturing of quantum nodes. This task not only entails qubit and device production but also the packaging of efficient optical and microwave signals to and from many independent color centers at once.

Optical technologies such as photonic integrated circuits (PICs) may play an important role in addressing these challenges. Their programmability[230] and access to a large number of spatial modes[231] are especially of interest to quantum network applications. Similar to their bulk optics counterparts, PICs comprise of low-loss on-chip components, such as waveguides, filters and switches. References 230–233 review the device concepts and state of the art of PIC technologies that may be relevant to quantum network applications. Driven by foundry adoption, as well as new frontiers in data communication,[234,235] photonic processors,[236,237] and optical quantum computing,[238] integrated photonic circuits have advanced dramatically in manufacturability and complexity over the last decade. The first notable feature of PICs for quantum technologies is their compact footprint, which not only promotes dense integration but also reduces phase errors in quantum interference of photons.[230] Next, phase modulators in PICs can implement on-chip switches for routing photons within an optical network,[230] and material nonlinearities can be used for efficient frequency conversion between visible and telecommunication photons.[239] Finally, multi-channel optical access can be accomplished using standard fiber arrays, and electrical packaging for large-scale control of color centers can be achieved using potential metal layers in a PIC stack.

Photonic circuits in diamond have been previously demonstrated for opto-mechanics[175] and nonlinear optics.[240] Gallium phosphide-on-diamond photonics have also been used to route the emission from NV centers.[160] However, the non-deterministic creation and integration of color centers in devices as well as the absence of single-crystal diamond wafers have limited the scale of diamond integrated photonics (see Sec. VII). One way to combine the functionalities and performance of industry-leading photonic circuits with diamond is through heterogeneous integration of diamond with other material systems. Also known as "hybrid photonics,"[241,242] this approach is akin to modern integrated circuits in that discrete chips are separately optimized and fabricated and then populated into a larger circuit board. Examples of heterogeneous integration include modulators and lasers in silicon photonics.[243] In the context of quantum photonics, recent successes include quantum emitters[241,242] and single-photon detectors,[244] which are otherwise difficult to achieve in a single material platform with high performance.

Heterogeneous integration of diamond color centers with PICs circumvents the yield issues associated with all-diamond architectures, thereby allowing potentially many addressable qubits within a single chip. A recent result showing the large-scale integration of color centers in diamond with hybrid photonic integrated circuits[58] is shown in Figs. 8(a)–8(c). Diamond quantum micro-chiplets, each consisting of eight diamond nanophotonic waveguides with at least one addressable group-IV color center, are integrated with PICs based on aluminum nitride [Fig. 8(c)]. After fabrication using the quasi-isotropic undercut technique (see Sec. VII), a total of 16 chiplets numbering to 128 waveguides were positioned with sub-micrometers accuracy on the PIC [Fig. 8(a)] using a pick-and-place technique [Fig. 8(b)]. The coupling of the color center to the waveguide can be as high as 55%, and the diamond-PIC coupling and PIC-to-optical fiber coupling are reported to be 34% and 11%, respectively. In addition, electrodes in this hybrid PIC enabled the *in situ* tuning of optical transition frequencies within this integrated device architecture.[58] The availability of multiple color centers per waveguide potentially allows for spectral multiplexing,[245,246] which is a hardware-efficient path to multiplying the total number of qubits to $N_s \times N_f$, where N_s and N_f are the number of spatial and frequency channels, respectively.

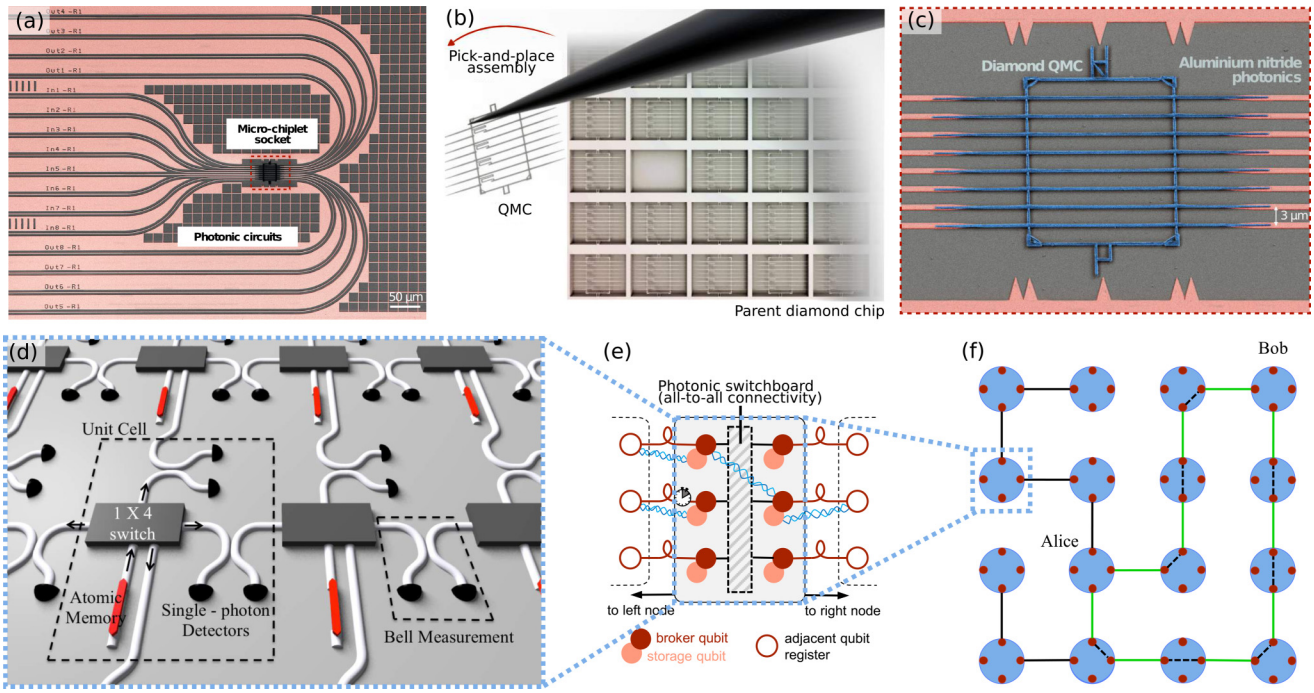

FIG. 8. Schematic of realized and envisioned architectures for large-scale hybrid integrated circuits enabling entanglement routing. (a) False-color SEM image of a AlN-on-sapphire photonic integrated circuit (PIC), containing a diamond quantum microchiplet [QMC, red dashed area, enlarged view in (c)]. These microchiplets with embedded color centers are pre-fabricated and -characterized in the diamond host material, and transferred onto the PIC using a pick-and-place technique (b), allowing to optimize PICs and microchiplets separately. This technique has been used to generate a defect-free array of 128 nanophotonic waveguides containing individually addressable quantum emitters, coupled to the PIC. Images (a)–(c) adapted with permission from Wan *et al.*, Nature **583**, 226–231 (2020). Copyright 2020 Springer Nature.[58] (d) Integrated multi-quantum memory node in a modular architecture.[41] Each unit cell (black dashed line) contains a diamond-based atomic memory (red), a fast, reconfigurable switching network allowing all-to-all connectivity (realized, e.g., via Mach–Zehnder interferometers), and photo-detectors. The atomic memory includes one communication and several memory qubits, with the communication qubit coupled to a diamond nanophotonic structure. Figure reprinted with permission from Choi *et al.*, npj Q. Inform. **5**, 104 (2019). Copyright 2019 Author(s), licensed under creativecommons.org/licenses/by/4.0/legalcode.[41] (e) Entanglement routing in a quantum network. A multi-path routing algorithm (realized, e.g., via re-configurable PICs, dashed black box) can improve the entanglement generation rate (wiggled blue lines) between distant nodes (white circles), compared to a linear repeater topology.[220] This allows concurrent communication links with only local information used in each node [(f), data and communication qubits depicted in light and dark red, respectively]. (e) adapted with permission from Ref. 220. (f) reprinted with permission from Pant *et al.*, npj Q. Inform. **5**, 1–9 (2019). Copyright 2019 Author(s), licensed under creativecommons.org/licenses/by/4.0/legalcode.[221]

With further improvements in waveguide-emitter coupling as well as diamond-nanocavity integration with PICs, such a hybrid architecture could become an important building block of future quantum network nodes. Looking forward, we expect future developments to also focus on integrating chip components for color center technologies, such as CMOS-integrated microwave electronics for spin control,[247] on-chip beam splitters for photon quantum interference,[238] optical switches for channel connectivity,[230] single-photon detectors[244,248–250] for heralded entanglement, and quantum frequency conversion[251,252] or frequency tuning[253] on the same micro-photonic platform. While these functionalities have been realized in other PIC platforms, a key challenge is to bring together various technologies and materials for implementing a chip-based node. Here, the advances in heterogeneous integration will be critical for controlling and deploying a large number of such chips.

As an example of such a chip, Fig. 8(d) shows a modular architecture with many unit cells per network node.[41] Each unit cell consists of atomic memories, photonic switches, and single-photon detectors. The atomic memories include communication qubits for inter-cell entanglement and memory qubits for long-term storage and intracell information processing. The switching network selects one of the adjacent cells, and the photo-detectors herald successful entanglement events between cells. Such a photonic architecture could allow for entanglement routing within a chip-based node, potentially boosting the communication rate.[9,220] By establishing connectivity between unit cells using optical switches, the resulting network is scalable because adding nodes does not require any modification in the existing network.

Once multiple long-lived memory qubits that can be controlled with high fidelity are available per quantum network node, the entanglement fidelity can be greatly improved through entanglement distillation (purification), where low fidelity entangled pairs are employed as a resource and transformed to a smaller number of high-fidelity pairs after local operations and classical communication.[254,255] Such a

scheme has recently been demonstrated in a proof-of-principle experiment between two distant NV centers that each have access to an additional ^{13}C memory.[38] While such distillation requires additional time resources as a result of two-way-classical-communication, quantum error correction[256] can achieve a more favorable key rate per qubit scaling.[229] Such an error correction can be performed if the operational error is smaller than the threshold of a given code [e.g., ≈ 0.189 for the Calderbank–Shor–Stean (CSS) code[257]]. If the photon loss of a link is sufficiently small, heralded entanglement generation can also be replaced with error correction, allowing to move beyond two-way signaling associated with the heralding.[258] In addition, multi-qubit network nodes can be operated in a way that outperforms more simple linear repeater schemes. For example, Fig. 8(f) shows a 2D network with nearest-neighbor connectivity that allows multi-path entanglement routing.[221] Crucially, the algorithm only requires local knowledge about which of the entanglement generation attempts with its nearest neighbor succeeded while still achieving faster key distribution than a linear repeater chain.[221]

IX. CONCLUSIONS

We have provided a Perspective on the emerging field of quantum networks based on diamond color centers. Diamond color centers already define the state of the art in multi-node entanglement-based networks[39] and in memory-enhanced quantum key distribution.[23] We expect the coming years to see rapid progress on photonic interfaces and integration of color centers, paving the way for first experiments on long-distance quantum links. From the basic building blocks, larger-scale devices will be designed and constructed. Control layers of higher abstraction—akin to the current Internet—are currently being developed.[259,260]

A future functional quantum network will support many interesting applications, such as distributed quantum computing,[261] accessing a quantum server in the cloud with full privacy,[262] and stabilizing quantum clocks.[43,263] Color centers in diamond may play an essential role in these networks, as the "satisfactory repeater," or perhaps the "transistor of the quantum age."

ACKNOWLEDGMENTS

We thank Ben Dixon, Mihir Bhaskar, Eric Bersin, Johannes Borregaard, Tim Taminiau, Matteo Pompili, and Matteo Pasini for feedback on the manuscript; Hans Beukers for the calculations of operation temperatures of color centers; and Matteo Pompili, Mihir Bhaskar, Christian Nguyen, Daniel Riedel, Alison Rugar, Shahriar Aghaeimeibodi, Conor Bradley, Mihir Pant, Yuan Lee, Michael Burek, and Cleaven Chia for providing originals of figures. D.E. acknowledges support from the Brookhaven National Laboratory, which is supported by the U.S. Department of Energy, Office of Basic Energy Sciences, under Contract No. DE-SC0012704. N.H.W. acknowledges support from the MITRE Quantum Moonshot initiative. H.C. acknowledges the Claude E. Shannon Fellowship and Samsung Scholarship. R.H. and M.R. acknowledge financial support from the EU Flagship on Quantum Technologies through the project Quantum Internet Alliance, from the Netherlands Organisation for Scientific Research (NWO) through a VICI grant and the Zwaartekracht program Quantum Software Consortium, the European Research Council (ERC) through a Consolidator Grant, and the joint research program "Modular quantum computers" by Fujitsu Limited and Delft University of Technology, co-funded by the Netherlands Enterprise Agency under Project No. PPS2007.

DATA AVAILABILITY

Data sharing is not applicable to this article as no new data were created or analyzed in this study.

REFERENCES

[1]J. Gertner, *The Idea Factory* (Penguin, New York, 2012).
[2]J. L. Park, "The concept of transition in quantum mechanics," Found. Phys. **1**, 23–33 (1970).
[3]H. J. Kimble, "The quantum internet," Nature **453**, 1023–1030 (2008).
[4]S. Wehner, D. Elkouss, and R. Hanson, "Quantum internet: A vision for the road ahead," Science **362**, 303 (2018).
[5]S. Pirandola, R. Laurenza, C. Ottaviani, and L. Banchi, "Fundamental limits of repeaterless quantum communications," Nat. Commun. **8**, 1–15 (2017).
[6]H.-J. Briegel, W. Dür, J. I. Cirac, and P. Zoller, "Quantum repeaters: The role of imperfect local operations in quantum communication," Phys. Rev. Lett. **81**, 5932–5935 (1998).
[7]C. Cabrillo, J. I. Cirac, P. García-Fernández, and P. Zoller, "Creation of entangled states of distant atoms by interference," Phys. Rev. A **59**, 1025–1033 (1999).
[8]S. D. Barrett and P. Kok, "Efficient high-fidelity quantum computation using matter qubits and linear optics," Phys. Rev. A **71**, 060310 (2005).
[9]L. M. Duan and H. J. Kimble, "Scalable photonic quantum computation through cavity-assisted interactions," Phys. Rev. Lett. **92**, 127902 (2004).
[10]A. Delteil, Z. Sun, W. B. Gao, E. Togan, S. Faelt, and A. Imamoglu, "Generation of heralded entanglement between distant hole spins," Nat. Phys. **12**, 218–223 (2016).
[11]R. Stockill, M. J. Stanley, L. Huthmacher, E. Clarke, M. Hugues, A. J. Miller, C. Matthiesen, C. Le Gall, and M. Atatúre, "Phase-tuned entangled state generation between distant spin qubits," Phys. Rev. Lett. **119**, 010503 (2017).
[12]D. L. Moehring, P. Maunz, S. Olmschenk, K. C. Younge, D. N. Matsukevich, L. M. Duan, and C. Monroe, "Entanglement of single-atom quantum bits at a distance," Nature **449**, 68–71 (2007).
[13]D. Hucul, I. V. Inlek, G. Vittorini, C. Crocker, S. Debnath, S. M. Clark, and C. Monroe, "Modular entanglement of atomic qubits using photons and phonons," Nat. Phys. **11**, 37–42 (2015).
[14]L. J. Stephenson, D. P. Nadlinger, B. C. Nichol, S. An, P. Drmota, T. G. Ballance, K. Thirumalai, J. F. Goodwin, D. M. Lucas, and C. J. Ballance, "High-rate, high-fidelity entanglement of qubits across an elementary quantum network," Phys. Rev. Lett. **124**, 110501 (2020).
[15]S. Ritter, C. Nölleke, C. Hahn, A. Reiserer, A. Neuzner, M. Uphoff, M. Mücke, E. Figueroa, J. Bochmann, and G. Rempe, "An elementary quantum network of single atoms in optical cavities," Nature **484**, 195–200 (2012).
[16]J. Hofmann, M. Krug, N. Ortegel, L. Gérard, M. Weber, W. Rosenfeld, and H. Weinfurter, "Heralded entanglement between widely separated atoms," Science **337**, 72–75 (2012).
[17]S. Daiss, S. Langenfeld, S. Welte, E. Distante, P. Thomas, L. Hartung, O. Morin, and G. Rempe, "A quantum-logic gate between distant quantum-network modules," Science **371**, 614–617 (2021).
[18]S. Langenfeld, S. Welte, L. Hartung, S. Daiss, P. Thomas, O. Morin, E. Distante, and G. Rempe, "Quantum teleportation between remote qubit memories with only a single photon as a resource," Phys. Rev. Lett. **126**, 130502 (2021).
[19]H. Bernien, B. Hensen, W. Pfaff, G. Koolstra, M. S. Blok, L. Robledo, T. H. Taminiau, M. Markham, D. J. Twitchen, L. Childress, and R. Hanson,

"Heralded entanglement between solid-state qubits separated by three metres," Nature **497**, 86–90 (2013).
[20]B. Hensen, H. Bernien, A. E. Dréau, A. Reiserer, N. Kalb, M. S. Blok, J. Ruitenberg, R. F. Vermeulen, R. N. Schouten, C. Abellán, W. Amaya, V. Pruneri, M. W. Mitchell, M. Markham, D. J. Twitchen, D. Elkouss, S. Wehner, T. H. Taminiau, and R. Hanson, "Loophole-free bell inequality violation using electron spins separated by 1.3 kilometres," Nature **526**, 682–686 (2015).
[21]M. K. Bhaskar, D. D. Sukachev, A. Sipahigil, R. E. Evans, M. J. Burek, C. T. Nguyen, L. J. Rogers, P. Siyushev, M. H. Metsch, H. Park, F. Jelezko, M. Lončar, and M. D. Lukin, "Quantum nonlinear optics with a germanium-vacancy color center in a nanoscale diamond waveguide," Phys. Rev. Lett. **118**, 223603 (2017).
[22]C. T. Nguyen, D. D. Sukachev, M. K. Bhaskar, B. Machielse, D. S. Levonian, E. N. Knall, P. Stroganov, R. Riedinger, H. Park, M. Lončar, and M. D. Lukin, "Quantum network nodes based on diamond qubits with an efficient nanophotonic interface," Phys. Rev. Lett. **123**, 183602 (2019).
[23]M. K. Bhaskar, R. Riedinger, B. Machielse, D. S. Levonian, C. T. Nguyen, E. N. Knall, H. Park, D. Englund, M. Lončar, D. D. Sukachev, and M. D. Lukin, "Experimental demonstration of memory-enhanced quantum communication," Nature **580**, 60–64 (2020).
[24]M. E. Trusheim, B. Pingault, N. H. Wan, M. Gündoğan, L. De Santis, R. Debroux, D. Gangloff, C. Purser, K. C. Chen, M. Walsh, J. J. Rose, J. N. Becker, B. Lienhard, E. Bersin, I. Paradeisanos, G. Wang, D. Lyzwa, A. R. Montblanch, G. Malladi, H. Bakhru, A. C. Ferrari, I. A. Walmsley, M. Atatüre, and D. Englund, "Transform-limited photons from a coherent tin-vacancy spin in diamond," Phys. Rev. Lett. **124**, 023602 (2020).
[25]S. A. Zargaleh, S. Hameau, B. Eble, F. Margaillan, H. J. von Bardeleben, J. L. Cantin, and W. Gao, "Nitrogen vacancy center in cubic silicon carbide: A promising qubit in the 1.5 um spectral range for photonic quantum networks," Phys. Rev. B **98**, 165203 (2018).
[26]R. Nagy, M. Niethammer, M. Widmann, Y.-C. Chen, P. Udvarhelyi, C. Bonato, J. U. Hassan, R. Karhu, I. G. Ivanov, N. T. Son, J. R. Maze, T. Ohshima, Ö. O. Soykal, Á. Gali, S.-Y. Lee, F. Kaiser, and J. Wrachtrup, "High-fidelity spin and optical control of single silicon-vacancy centres in silicon carbide," Nat. Commun. **10**, 1954 (2019).
[27]A. Bourassa, C. P. Anderson, K. C. Miao, M. Onizhuk, H. Ma, A. L. Crook, H. Abe, J. Ul-Hassan, T. Ohshima, N. T. Son, G. Galli, and D. D. Awschalom, "Entanglement and control of single nuclear spins in isotopically engineered silicon carbide," Nat. Mater. **19**, 1319–1325 (2020).
[28]D. M. Lukin, M. A. Guidry, and J. Vučković, "Integrated quantum photonics with silicon carbide: Challenges and prospects," PRX Q. **1**, 020102 (2020).
[29]J.-F. Wang, F.-F. Yan, Q. Li, Z.-H. Liu, H. Liu, G.-P. Guo, L.-P. Guo, X. Zhou, J.-M. Cui, J. Wang, Z.-Q. Zhou, X.-Y. Xu, J.-S. Xu, C.-F. Li, and G.-C. Guo, "Coherent control of nitrogen-vacancy center spins in silicon carbide at room temperature," Phys. Rev. Lett. **124**, 223601 (2020).
[30]M. Raha, S. Chen, C. M. Phenicie, S. Ourari, A. M. Dibos, and J. D. Thompson, "Optical quantum nondemolition measurement of a single rare earth ion qubit," Nat. Commun. **11**, 1605 (2020).
[31]J. M. Kindem, A. Ruskuc, J. G. Bartholomew, J. Rochman, Y. Q. Huan, and A. Faraon, "Control and single-shot readout of an ion embedded in a nanophotonic cavity," Nature **580**, 201–204 (2020).
[32]B. Merkel, A. Ulanowski, and A. Reiserer, "Coherent and Purcell-enhanced emission from erbium dopants in a cryogenic high-Q resonator," Phys. Rev. X **10**, 041025 (2020).
[33]Y. Chu and S. Gröblacher, "A perspective on hybrid quantum opto- and electromechanical systems," Appl. Phys. Lett. **117**, 150503 (2020).
[34]M. Mirhosseini, A. Sipahigil, M. Kalaee, and O. Painter, "Superconducting qubit to optical photon transduction," Nature **588**, 599–603 (2020).
[35]M. Forsch, R. Stockill, A. Wallucks, I. Marinković, C. Gärtner, R. A. Norte, F. van Otten, A. Fiore, K. Srinivasan, and S. Gröblacher, "Microwave-to-optics conversion using a mechanical oscillator in its quantum ground state," Nat. Phys. **16**, 69–74 (2020).
[36]W. Hease, A. Rueda, R. Sahu, M. Wulf, G. Arnold, H. G. Schwefel, and J. M. Fink, "Bidirectional electro-optic wavelength conversion in the quantum ground state," PRX Q. **1**, 020315 (2020).
[37]S. Krastanov, H. Raniwala, J. Holzgrafe, K. Jacobs, M. Lončar, M. J. Reagor, and D. R. Englund, "Optically-heralded entanglement of superconducting systems in quantum networks," arXiv:2012.13408 (2020).
[38]N. Kalb, A. A. Reiserer, P. C. Humphreys, J. J. Bakermans, S. J. Kamerling, N. H. Nickerson, S. C. Benjamin, D. J. Twitchen, M. Markham, and R. Hanson, "Entanglement distillation between solid-state quantum network nodes," Science **356**, 928–932 (2017).
[39]M. Pompili, S. L. N. Hermans, S. Baier, H. K. C. Beukers, P. C. Humphreys, R. N. Schouten, R. F. L. Vermeulen, M. J. Tiggelman, L. dos Santos Martins, B. Dirkse, S. Wehner, and R. Hanson, "Realization of a multinode quantum network of remote solid-state qubits," Science **372**, 259–264 (2021).
[40]N. H. Nickerson, J. F. Fitzsimons, and S. C. Benjamin, "Freely scalable quantum technologies using cells of 5-to-50 qubits with very lossy and noisy photonic links," Phys. Rev. X **4**, 041041 (2014).
[41]H. Choi, M. Pant, S. Guha, and D. Englund, "Percolation-based architecture for cluster state creation using photon-mediated entanglement between atomic memories," npj Q. Inform. **5**, 104 (2019).
[42]D. Gottesman, T. Jennewein, and S. Croke, "Longer-baseline telescopes using quantum repeaters," Phys. Rev. Lett. **109**, 070503 (2012).
[43]P. Kómár, E. M. Kessler, M. Bishof, L. Jiang, A. S. Sørensen, J. Ye, and M. D. Lukin, "A quantum network of clocks," Nat. Phys. **10**, 582–587 (2014).
[44]A. Ekert and R. Renner, "The ultimate physical limits of privacy," Nature **507**, 443–447 (2014).
[45]P. C. Humphreys, N. Kalb, J. P. Morits, R. N. Schouten, R. F. Vermeulen, D. J. Twitchen, M. Markham, and R. Hanson, "Deterministic delivery of remote entanglement on a quantum network," Nature **558**, 268–273 (2018).
[46]T. H. Taminiau, J. Cramer, T. Van Der Sar, V. V. Dobrovitski, and R. Hanson, "Universal control and error correction in multi-qubit spin registers in diamond," Nat. Nanotechnol. **9**, 171–176 (2014).
[47]M. H. Abobeih, J. Cramer, M. A. Bakker, N. Kalb, M. Markham, D. J. Twitchen, and T. H. Taminiau, "One-second coherence for a single electron spin coupled to a multi-qubit nuclear-spin environment," Nat. Commun. **9**, 2552 (2018).
[48]A. Reiserer, N. Kalb, M. S. Blok, K. J. M. van Bemmelen, T. H. Taminiau, R. Hanson, D. J. Twitchen, and M. Markham, "Robust quantum-network memory using decoherence-protected subspaces of nuclear spins," Phys. Rev. X **6**, 021040 (2016).
[49]N. Kalb, P. C. Humphreys, J. J. Slim, and R. Hanson, "Dephasing mechanisms of diamond-based nuclear-spin memories for quantum networks," Phys. Rev. A **97**, 062330 (2018).
[50]C. T. Nguyen, D. D. Sukachev, M. K. Bhaskar, B. Machielse, D. S. Levonian, E. N. Knall, P. Stroganov, C. Chia, M. J. Burek, R. Riedinger, H. Park, M. Lončar, and M. D. Lukin, "An integrated nanophotonic quantum register based on silicon-vacancy spins in diamond," Phys. Rev. B **100**, 165428 (2019).
[51]R. E. Evans, M. K. Bhaskar, D. D. Sukachev, C. T. Nguyen, A. Sipahigil, M. J. Burek, B. Machielse, G. H. Zhang, A. S. Zibrov, E. Bielejec, H. Park, M. Lončar, and M. D. Lukin, "Photon-mediated interactions between quantum emitters in a diamond nanocavity," Science **362**, 662–665 (2018).
[52]A. Sipahigil, R. E. Evans, D. D. Sukachev, M. J. Burek, J. Borregaard, M. K. Bhaskar, C. T. Nguyen, J. L. Pacheco, H. A. Atikian, C. Meuwly, R. M. Camacho, F. Jelezko, E. Bielejec, H. Park, M. Lončar, and M. D. Lukin, "An integrated diamond nanophotonics platform for quantum-optical networks," Science **354**, 847–850 (2016).
[53]B. Machielse, S. Bogdanovic, S. Meesala, S. Gauthier, M. J. Burek, G. Joe, M. Chalupnik, Y. I. Sohn, J. Holzgrafe, R. E. Evans, C. Chia, H. Atikian, M. K. Bhaskar, D. D. Sukachev, L. Shao, S. Maity, M. D. Lukin, and M. Lončar, "Quantum interference of electromechanically stabilized emitters in nanophotonic devices," Phys. Rev. X **9**, 031022 (2019).
[54]D. D. Sukachev, A. Sipahigil, C. T. Nguyen, M. K. Bhaskar, R. E. Evans, F. Jelezko, and M. D. Lukin, "Silicon-vacancy spin qubit in diamond: A quantum

memory exceeding 10 ms with single-shot state readout," Phys. Rev. Lett. **119**, 223602 (2017).
[55]M. H. Metsch, K. Senkalla, B. Tratzmiller, J. Scheuer, M. Kern, J. Achard, A. Tallaire, M. B. Plenio, P. Siyushev, and F. Jelezko, "Initialization and readout of nuclear spins via a negatively charged silicon-vacancy center in diamond," Phys. Rev. Lett. **122**, 190503 (2019).
[56]C. T. Nguyen, D. D. Sukachev, M. K. Bhaskar, B. MacHielse, D. S. Levonian, E. N. Knall, P. Stroganov, C. Chia, M. J. Burek, R. Riedinger, H. Park, M. Lončar, and M. D. Lukin, "An integrated nanophotonic quantum register based on silicon-vacancy spins in diamond," Phys. Rev. B **100**, 165428 (2019).
[57]Y. I. Sohn, S. Meesala, B. Pingault, H. A. Atikian, J. Holzgrafe, M. Gündoğ˘an, C. Stavrakas, M. J. Stanley, A. Sipahigil, J. Choi, M. Zhang, J. L. Pacheco, J. Abraham, E. Bielejec, M. D. Lukin, M. Atatüre, and M. Lončar, "Controlling the coherence of a diamond spin qubit through its strain environment," Nat. Commun. **9**, 17–22 (2018).
[58]N. H. Wan, T. J. Lu, K. C. Chen, M. P. Walsh, M. E. Trusheim, L. De Santis, E. A. Bersin, I. B. Harris, S. L. Mouradian, I. R. Christen, E. S. Bielejec, and D. Englund, "Large-scale integration of artificial atoms in hybrid photonic circuits," Nature **583**, 226–231 (2020).
[59]E. Neu, M. Agio, and C. Becher, "Photophysics of single silicon vacancy centers in diamond: Implications for single photon emission," Opt. Express. **20**, 19956 (2012).
[60]J. Riedrich-Möller, C. Arend, C. Pauly, F. Mücklich, M. Fischer, S. Gsell, M. Schreck, and C. Becher, "Deterministic coupling of a single silicon-vacancy color center to a photonic crystal cavity in diamond," Nano Lett. **14**, 5281–5287 (2014).
[61]E. Neu, D. Steinmetz, J. Riedrich-Möller, S. Gsell, M. Fischer, M. Schreck, and C. Becher, "Single photon emission from silicon-vacancy colour centres in chemical vapour deposition nano-diamonds on iridium," New J. Phys. **13**, 025012 (2011).
[62]A. Dietrich, K. D. Jahnke, J. M. Binder, T. Teraji, J. Isoya, L. J. Rogers, and F. Jelezko, "Isotopically varying spectral features of silicon-vacancy in diamond," New J. Phys. **16**, 113019 (2014).
[63]L. Rogers, K. Jahnke, T. Teraji, L. Marseglia, C. Müller, B. Naydenov, H. Schauffert, C. Kranz, J. Isoya, L. McGuinness, and F. Jelezko, "Multiple intrinsically identical single-photon emitters in the solid state," Nat. Commun. **5**, 4739 (2014).
[64]C. Hepp, T. Müller, V. Waselowski, J. N. Becker, B. Pingault, H. Sternschulte, D. Steinmüller-Nethl, A. Gali, J. R. Maze, M. Atatüre, and C. Becher, "Electronic structure of the silicon vacancy color center in diamond," Phys. Rev. Lett. **112**, 036405 (2014).
[65]B. Pingault, D. D. Jarausch, C. Hepp, L. Klintberg, J. N. Becker, M. Markham, C. Becher, and M. Atatüre, "Coherent control of the silicon-vacancy spin in diamond," Nat. Commun. **8**, 15579 (2017).
[66]T. Iwasaki, F. Ishibashi, Y. Miyamoto, Y. Doi, S. Kobayashi, T. Miyazaki, K. Tahara, K. D. Jahnke, L. J. Rogers, B. Naydenov, F. Jelezko, S. Yamasaki, S. Nagamachi, T. Inubushi, N. Mizuochi, and M. Hatano, "Germanium-vacancy single color centers in diamond," Sci. Rep. **5**, 12882 (2015).
[67]R. Høy Jensen, E. Janitz, Y. Fontana, Y. He, O. Gobron, I. P. Radko, M. Bhaskar, R. Evans, C. D. Rodríguez Rosenblueth, L. Childress, A. Huck, and U. Lund Andersen, "Cavity-enhanced photon emission from a single germanium-vacancy center in a diamond membrane," Phys. Rev. Appl. **13**, 064016 (2020).
[68]M. Nguyen, N. Nikolay, C. Bradac, M. Kianinia, E. A. Ekimov, N. Mendelson, O. Benson, and I. Aharonovich, "Photodynamics and quantum efficiency of germanium vacancy color centers in diamond," Adv. Photonics **1**, 066002 (2019).
[69]P. Siyushev, M. H. Metsch, A. Ijaz, J. M. Binder, M. K. Bhaskar, D. D. Sukachev, A. Sipahigil, R. E. Evans, C. T. Nguyen, M. D. Lukin, P. R. Hemmer, Y. N. Palyanov, I. N. Kupriyanov, Y. M. Borzdov, L. J. Rogers, and F. Jelezko, "Optical and microwave control of germanium-vacancy center spins in diamond," Phys. Rev. B **96**, 081201 (2017).
[70]T. Iwasaki, Y. Miyamoto, T. Taniguchi, P. Siyushev, M. H. Metsch, F. Jelezko, and M. Hatano, "Tin-vacancy quantum emitters in diamond," Phys. Rev. Lett. **119**, 253601 (2017).
[71]J. Görlitz, D. Herrmann, G. Thiering, P. Fuchs, M. Gandil, T. Iwasaki, T. Taniguchi, M. Kieschnick, J. Meijer, M. Hatano, A. Gali, and C. Becher, "Spectroscopic investigations of negatively charged tin-vacancy centres in diamond," New J. Phys. **22**, 013048 (2020).
[72]S. D. Tchernij, T. Herzig, J. Forneris, J. Küpper, S. Pezzagna, P. Traina, E. Moreva, I. P. Degiovanni, G. Brida, N. Skukan, M. Genovese, M. Jakšić, J. Meijer, and P. Olivero, "Single-photon-emitting optical centers in diamond fabricated upon Sn implantation," ACS Photonics **4**, 2580–2586 (2017).
[73]A. E. Rugar, S. Aghaeimeibodi, D. Riedel, C. Dory, H. Lu, P. J. McQuade, Z.-X. Shen, N. A. Melosh, and J. Vučković, "Quantum photonic interface for tin-vacancy centers in diamond," Phys. Rev. X **11**, 031021 (2021).
[74]M. E. Trusheim, N. H. Wan, K. C. Chen, C. J. Ciccarino, J. Flick, R. Sundararaman, G. Malladi, E. Bersin, M. Walsh, B. Lienhard, H. Bakhru, P. Narang, and D. Englund, "Lead-related quantum emitters in diamond," Phys. Rev. B **99**, 075430 (2019).
[75]S. Ditalia Tchernij, T. Lúhmann, T. Herzig, J. Küpper, A. Damin, S. Santonocito, M. Signorile, P. Traina, E. Moreva, F. Celegato, S. Pezzagna, I. P. Degiovanni, P. Olivero, M. Jakšić, J. Meijer, P. M. Genovese, and J. Forneris, "Single-photon emitters in lead-implanted single-crystal diamond," ACS Photonics **5**, 4864–4871 (2018).
[76]J. E. Fröch, A. Bahm, M. Kianinia, Z. Mu, V. Bhatia, S. Kim, J. M. Cairney, W. Gao, C. Bradac, I. Aharonovich, and M. Toth, "Versatile direct-writing of dopants in a solid state host through recoil implantation," Nat. Commun. **11**, 5039 (2020).
[77]P. Wang, T. Taniguchi, Y. Miyamoto, and M. Hatano, "Low-temperature spectroscopic investigation of lead-vacancy centers in diamond fabricated by high-pressure and high-temperature treatment," arXiv::2106.03413 (2021).
[78]M. W. Doherty, N. B. Manson, P. Delaney, F. Jelezko, J. Wrachtrup, and L. C. Hollenberg, "The nitrogen-vacancy colour centre in diamond," Phys. Rep. **528**, 1–45 (2013).
[79]I. P. Radko, M. Boll, N. M. Israelsen, N. Raatz, J. Meijer, F. Jelezko, U. L. Andersen, and A. Huck, "Determining the internal quantum efficiency of shallow-implanted nitrogen-vacancy defects in bulk diamond," Opt. Express. **24**, 27715 (2016).
[80]A. Faraon, P. E. Barclay, C. Santori, K. M. C. Fu, and R. G. Beausoleil, "Resonant enhancement of the zero-phonon emission from a colour centre in a diamond cavity," Nat. Photonics **5**, 301–305 (2011).
[81]D. Riedel, I. Söllner, B. J. Shields, S. Starosielec, P. Appel, E. Neu, P. Maletinsky, and R. J. Warburton, "Deterministic enhancement of coherent photon generation from a nitrogen-vacancy center in ultrapure diamond," Phys. Rev. X **7**, 031040 (2017).
[82]M. Ruf, M. Weaver, S. van Dam, and R. Hanson, "Resonant excitation and Purcell enhancement of coherent nitrogen-vacancy centers coupled to a Fabry–Pérot microcavity," Phys. Rev. Appl. **15**, 024049 (2021).
[83]C. Hepp, "Electronic structure of the silicon vacancy color center in diamond," Ph.D. thesis (Saarland University, 2014).
[84]C. Bradac, W. Gao, J. Forneris, M. E. Trusheim, and I. Aharonovich, "Quantum nanophotonics with group IV defects in diamond," Nat. Commun. **10**, 5625 (2019).
[85]A. Pershin, G. Barcza, Ö. Legeza, and A. Gali, "Highly tunable magneto-optical response from magnesium-vacancy color centers in diamond," npj Q. Inform. **7**, 99 (2021).
[86]H. Bernien, L. Childress, L. Robledo, M. Markham, D. Twitchen, and R. Hanson, "Two-photon quantum interference from separate nitrogen vacancy centers in diamond," Phys. Rev. Lett. **108**, 043604 (2012).
[87]A. Faraon, C. Santori, Z. Huang, V. M. Acosta, and R. G. Beausoleil, "Coupling of nitrogen-vacancy centers to photonic crystal cavities in monocrystalline diamond," Phys. Rev. Lett. **109**, 033604 (2012).
[88]M. Ruf, M. IJspeert, S. van Dam, N. de Jong, H. van den Berg, G. Evers, and R. Hanson, "Optically coherent nitrogen-vacancy centers in micrometer-thin etched diamond membranes," Nano Lett. **19**, 3987–3992 (2019).
[89]T. Astner, J. Gugler, A. Angerer, S. Wald, S. Putz, N. J. Mauser, M. Trupke, H. Sumiya, S. Onoda, J. Isoya, J. Schmiedmayer, P. Mohn, and J. Majer,

"Solid-state electron spin lifetime limited by phononic vacuum modes," Nat. Mater. **17**, 313–317 (2018).
[90]L. De Santis, M. Trusheim, K. Chen, and D. Englund, "Investigation of the Stark effect on a centrosymmetric quantum emitter in diamond," arXiv:2102.01322 (2021).
[91]S. Aghaeimeibodi, D. Riedel, A. E. Rugar, C. Dory, and J. Vučković, "Electrical tuning of tin-vacancy centers in diamond," Phys. Rev. Appl. **15**, 064010 (2021).
[92]G. Thiering and A. Gali, "Ab initio magneto-optical spectrum of group-IV vacancy color centers in diamond," Phys. Rev. X **8**, 021063 (2018).
[93]A. J. Sigillito, H. Malissa, A. M. Tyryshkin, H. Riemann, N. V. Abrosimov, P. Becker, H.-J. Pohl, M. L. W. Thewalt, K. M. Itoh, J. J. L. Morton, A. A. Houck, D. I. Schuster, and S. A. Lyon, "Fast, low-power manipulation of spin ensembles in superconducting microresonators," Appl. Phys. Lett. **104**, 222407 (2014).
[94]K. D. Jahnke, A. Sipahigil, J. M. Binder, M. W. Doherty, M. Metsch, L. J. Rogers, N. B. Manson, M. D. Lukin, and F. Jelezko, "Electron–phonon processes of the silicon-vacancy centre in diamond," New J. Phys. **17**, 043011 (2015).
[95]S. Meesala, Y. I. Sohn, B. Pingault, L. Shao, H. A. Atikian, J. Holzgrafe, M. Gündoğan, C. Stavrakas, A. Sipahigil, C. Chia, R. Evans, M. J. Burek, M. Zhang, L. Wu, J. L. Pacheco, J. Abraham, E. Bielejec, M. D. Lukin, M. Atatüre, and M. Lončar, "Strain engineering of the silicon-vacancy center in diamond," Phys. Rev. B **97**, 205444 (2018).
[96]B. Pingault, J. N. Becker, C. H. Schulte, C. Arend, C. Hepp, T. Godde, A. I. Tartakovskii, M. Markham, C. Becher, and M. Atatüre, "All-optical formation of coherent dark states of silicon-vacancy spins in diamond," Phys. Rev. Lett. **113**, 263601 (2014).
[97]J. N. Becker, B. Pingault, D. Groß, M. Gündoğan, N. Kukharchyk, M. Markham, A. Edmonds, M. Atatüre, P. Bushev, and C. Becher, "All-optical control of the silicon-vacancy spin in diamond at millikelvin temperatures," Phys. Rev. Lett. **120**, 053603 (2018).
[98]S. Maity, L. Shao, S. Bogdanović, S. Meesala, Y.-I. Sohn, N. Sinclair, B. Pingault, M. Chalupnik, C. Chia, L. Zheng, K. Lai, and M. Lončar, "Coherent acoustic control of a single silicon vacancy spin in diamond," Nat. Commun. **11**, 193 (2020).
[99]J. Franck and E. G. Dymond, "Elementary processes of photochemical reactions," Trans. Faraday Soc. **21**, 536 (1926).
[100]E. Condon, "A theory of intensity distribution in band systems," Phys. Rev. **28**, 1182–1201 (1926).
[101]B. L. Green, S. Mottishaw, B. G. Breeze, A. M. Edmonds, U. F. S. D'Haenens-Johansson, M. W. Doherty, S. D. Williams, D. J. Twitchen, and M. E. Newton, "Neutral silicon-vacancy center in diamond: Spin polarization and lifetimes," Phys. Rev. Lett. **119**, 096402 (2017).
[102]B. C. Rose, D. Huang, Z.-H. Zhang, P. Stevenson, A. M. Tyryshkin, S. Sangtawesin, S. Srinivasan, L. Loudin, M. L. Markham, A. M. Edmonds, D. J. Twitchen, S. A. Lyon, and N. P. de Leon, "Observation of an environmentally insensitive solid-state spin defect in diamond," Science **361**, 60–63 (2018).
[103]B. L. Green, M. W. Doherty, E. Nako, N. B. Manson, U. F. S. D'Haenens-Johansson, S. D. Williams, D. J. Twitchen, and M. E. Newton, "Electronic structure of the neutral silicon-vacancy center in diamond," Phys. Rev. B **99**, 161112 (2019).
[104]Z.-H. Zhang, P. Stevenson, G. Thiering, B. C. Rose, D. Huang, A. M. Edmonds, M. L. Markham, S. A. Lyon, A. Gali, and N. P. de Leon, "Optically detected magnetic resonance in neutral silicon vacancy centers in diamond via bound exciton states," Phys. Rev. Lett. **125**, 237402 (2020).
[105]C. E. Bradley, J. Randall, M. H. Abobeih, R. C. Berrevoets, M. J. Degen, M. A. Bakker, M. Markham, D. J. Twitchen, and T. H. Taminiau, "A ten-qubit solid-state spin register with quantum memory up to one minute," Phys. Rev. X **9**, 31045 (2019).
[106]G. Waldherr, Y. Wang, S. Zaiser, M. Jamali, T. Schulte-Herbrüggen, H. Abe, T. Ohshima, J. Isoya, J. F. Du, P. Neumann, and J. Wrachtrup, "Quantum error correction in a solid-state hybrid spin register," Nature **506**, 204–207 (2014).
[107]J. Cramer, N. Kalb, M. A. Rol, B. Hensen, M. S. Blok, M. Markham, D. J. Twitchen, R. Hanson, and T. H. Taminiau, "Repeated quantum error correction on a continuously encoded qubit by real-time feedback," Nat. Commun. **7**, 11526 (2016).
[108]M. H. Abobeih, "From atomic-scale imaging to quantum fault-tolerance with spins in diamond," Ph.D. thesis (TU Delft, 2021).
[109]M. H. Abobeih, J. Randall, C. E. Bradley, H. P. Bartling, M. A. Bakker, M. J. Degen, M. Markham, D. J. Twitchen, and T. H. Taminiau, "Atomic-scale imaging of a 27-nuclear-spin cluster using a quantum sensor," Nature **576**, 411–415 (2019).
[110]K. Jung, M. H. Abobeih, J. Yun, G. Kim, H. Oh, A. Henry, T. H. Taminiau, and D. Kim, "Deep learning enhanced individual nuclear-spin detection," npj Q. Inform. **7**, 41 (2021).
[111]W. Pfaff, B. J. Hensen, H. Bernien, S. B. Van Dam, M. S. Blok, T. H. Taminiau, M. J. Tiggelman, R. N. Schouten, M. Markham, D. J. Twitchen, and R. Hanson, "Unconditional quantum teleportation between distant solid-state quantum bits," Science **345**, 532–535 (2014).
[112]H. P. Bartling, M. H. Abobeih, B. Pingault, M. J. Degen, S. J. H. Loenen, C. E. Bradley, J. Randall, M. Markham, D. J. Twitchen, and T. H. Taminiau, "Coherence and entanglement of inherently long-lived spin pairs in diamond," arXiv:2103.07961 (2021).
[113]M. Pfender, N. Aslam, H. Sumiya, S. Onoda, P. Neumann, J. Isoya, C. A. Meriles, and J. Wrachtrup, "Nonvolatile nuclear spin memory enables sensor-unlimited nanoscale spectroscopy of small spin clusters," Nat. Commun. **8**, 834 (2017).
[114]M. Pfender, P. Wang, H. Sumiya, S. Onoda, W. Yang, D. B. R. Dasari, P. Neumann, X.-y. Pan, J. Isoya, R.-b. Liu, and J. Wrachtrup, "High-resolution spectroscopy of single nuclear spins via sequential weak measurements," Nat. Commun. **10**, 594 (2019).
[115]M. J. Degen, S. J. H. Loenen, H. P. Bartling, C. E. Bradley, A. L. Meinsma, M. Markham, D. J. Twitchen, and T. H. Taminiau, "Entanglement of dark electron-nuclear spin defects in diamond," Nat. Commun. **12**, 3470 (2021).
[116]T. Yamamoto, C. Müller, L. P. McGuinness, T. Teraji, B. Naydenov, S. Onoda, T. Ohshima, J. Wrachtrup, F. Jelezko, and J. Isoya, "Strongly coupled diamond spin qubits by molecular nitrogen implantation," Phys. Rev. B **88**, 201201 (2013).
[117]M. J. Degen, "On the creation, coherence and entanglement of multi-defect quantum registers in diamond," Ph.D. thesis (TU Delft, 2021).
[118]A. S. Sørensen and K. Mølmer, "Probabilistic generation of entanglement in optical cavities," Phys. Rev. Lett. **90**, 127903 (2003).
[119]A. Reiserer and G. Rempe, "Cavity-based quantum networks with single atoms and optical photons," Rev. Mod. Phys. **87**, 1379–1418 (2015).
[120]K. C. Chen, E. Bersin, and D. Englund, "A polarization encoded photon-to-spin interface," npj Q. Inform. **7**, 1–6 (2021).
[121]T. Schröder, S. L. Mouradian, J. Zheng, M. E. Trusheim, M. Walsh, E. H. Chen, L. Li, I. Bayn, and D. Englund, "Quantum nanophotonics in diamond," J. Opt. Soc. Am. B **33**, B65 (2016).
[122]S. Johnson, P. R. Dolan, and J. M. Smith, "Diamond photonics for distributed quantum networks," Progress Q. Electron. **55**, 129–165 (2017).
[123]E. Janitz, M. K. Bhaskar, and L. Childress, "Cavity quantum electrodynamics with color centers in diamond," Optica **7**, 1232 (2020).
[124]J. P. Hadden, J. P. Harrison, A. C. Stanley-Clarke, L. Marseglia, Y.-L. D. Ho, B. R. Patton, J. L. O'Brien, and J. G. Rarity, "Strongly enhanced photon collection from diamond defect centers under microfabricated integrated solid immersion lenses," Appl. Phys. Lett. **97**, 241901 (2010).
[125]L. Marseglia, J. P. Hadden, A. C. Stanley-Clarke, J. P. Harrison, B. Patton, Y.-L. D. Ho, B. Naydenov, F. Jelezko, J. Meijer, P. R. Dolan, J. M. Smith, J. G. Rarity, and J. L. O'Brien, "Nanofabricated solid immersion lenses registered to single emitters in diamond," Appl. Phys. Lett. **98**, 133107 (2011).
[126]L. Robledo, L. Childress, H. Bernien, B. Hensen, P. F. A. Alkemade, and R. Hanson, "High-fidelity projective read-out of a solid-state spin quantum register," Nature **477**, 574–578 (2011).

[127]M. Jamali, I. Gerhardt, M. Rezai, K. Frenner, H. Fedder, and J. Wrachtrup, "Microscopic diamond solid-immersion-lenses fabricated around single defect centers by focused ion beam milling," Rev. Sci. Instrum. **85**, 123703 (2014).
[128]D. Riedel, D. Rohner, M. Ganzhorn, T. Kaldewey, P. Appel, E. Neu, R. J. Warburton, and P. Maletinsky, "Low-loss broadband antenna for efficient photon collection from a coherent spin in diamond," Phys. Rev. Appl. **2**, 064011 (2014).
[129]D. Chen, Z. Mu, Y. Zhou, J. E. Fröch, A. Rasmit, C. Diederichs, N. Zheludev, I. Aharonovich, and W.-b. Gao, "Optical gating of resonance fluorescence from a single germanium vacancy color center in diamond," Phys. Rev. Lett. **123**, 033602 (2019).
[130]N. H. Wan, B. J. Shields, D. Kim, S. Mouradian, B. Lienhard, M. Walsh, H. Bakhru, T. Schröder, and D. Englund, "Efficient extraction of light from a nitrogen-vacancy center in a diamond parabolic reflector," Nano Lett. **18**, 2787–2793 (2018).
[131]N. Hedrich, D. Rohner, M. Batzer, P. Maletinsky, and B. J. Shields, "Parabolic diamond scanning probes for single-spin magnetic field imaging," Phys. Rev. Appl. **14**, 064007 (2020).
[132]P. Maletinsky, S. Hong, M. S. Grinolds, B. Hausmann, M. D. Lukin, R. L. Walsworth, M. Loncar, and A. Yacoby, "A robust scanning diamond sensor for nanoscale imaging with single nitrogen-vacancy centres," Nat. Nanotechnol. **7**, 320–324 (2012).
[133]B. J. M. Hausmann, M. Khan, Y. Zhang, T. M. Babinec, K. Martinick, M. McCutcheon, P. R. Hemmer, and M. Loncar, "Fabrication of diamond nanowires for quantum information processing applications," Diam. Relat. Mater. **19**, 621–629 (2010).
[134]T. M. Babinec, B. J. Hausmann, M. Khan, Y. Zhang, J. R. Maze, P. R. Hemmer, and M. Lončar, "A diamond nanowire single-photon source," Nat. Nanotechnol. **5**, 195–199 (2010).
[135]S.-W. Jeon, J. Lee, H. Jung, S.-W. Han, Y.-W. Cho, Y.-S. Kim, H.-T. Lim, Y. Kim, M. Niethammer, W. C. Lim, J. Song, S. Onoda, T. Ohshima, R. Reuter, A. Denisenko, J. Wrachtrup, and S.-Y. Lee, "Bright nitrogen-vacancy centers in diamond inverted nanocones," ACS Photonics **7**, 2739–2747 (2020).
[136]J. T. Choy, I. Bulu, B. J. M. Hausmann, E. Janitz, I.-C. Huang, and M. Lončar, "Spontaneous emission and collection efficiency enhancement of single emitters in diamond via plasmonic cavities and gratings," Appl. Phys. Lett. **103**, 161101 (2013).
[137]L. Li, E. H. Chen, J. Zheng, S. L. Mouradian, F. Dolde, T. Schröder, S. Karaveli, M. L. Markham, D. J. Twitchen, and D. Englund, "Efficient photon collection from a nitrogen vacancy center in a circular bullseye grating," Nano Lett. **15**, 1493–1497 (2015).
[138]M. J. Burek, N. P. de Leon, B. J. Shields, B. J. M. Hausmann, Y. Chu, Q. Quan, A. S. Zibrov, H. Park, M. D. Lukin, and M. Lončar, "Free-standing mechanical and photonic nanostructures in single-crystal diamond," Nano Lett. **12**, 6084–6089 (2012).
[139]S. A. Momenzadeh, R. J. Stöhr, F. F. de Oliveira, A. Brunner, A. Denisenko, S. Yang, F. Reinhard, and J. Wrachtrup, "Nanoengineered diamond waveguide as a robust bright platform for nanomagnetometry using shallow nitrogen vacancy centers," Nano Lett. **15**, 165–169 (2015).
[140]B. J. Shields, Q. P. Unterreithmeier, N. P. de Leon, H. Park, and M. D. Lukin, "Efficient readout of a single spin state in diamond via spin-to-charge conversion," Phys. Rev. Lett. **114**, 136402 (2015).
[141]S. L. Mouradian, T. Schröder, C. B. Poitras, L. Li, J. Goldstein, E. H. Chen, M. Walsh, J. Cardenas, M. L. Markham, D. J. Twitchen, M. Lipson, and D. Englund, "Scalable integration of long-lived quantum memories into a photonic circuit," Phys. Rev. X **5**, 031009 (2015).
[142]R. N. Patel, T. Schröder, N. Wan, L. Li, S. L. Mouradian, E. H. Chen, and D. R. Englund, "Efficient photon coupling from a diamond nitrogen vacancy center by integration with silica fiber," Light: Sci. Appl. **5**, e16032 (2016).
[143]A. E. Rugar, C. Dory, S. Aghaeimeibodi, H. Lu, S. Sun, S. D. Mishra, Z.-X. Shen, N. A. Melosh, and J. Vučković, "Narrow-linewidth tin-vacancy centers in a diamond waveguide," ACS Photonics **7**, 2356–2361 (2020).
[144]T. Legero, T. Wilk, A. Kuhn, and G. Rempe, "Time-resolved two-photon quantum interference," Appl. Phys. B **77**, 797–802 (2003).
[145]T. Legero, T. Wilk, A. Kuhn, and G. Rempe, "Characterization of single photons using two-photon interference," Adv. Atom. Mol. Opt. Phys. **53**, 253–289 (2006).
[146]M. J. Burek, Y. Chu, M. S. Z. Liddy, P. Patel, J. Rochman, S. Meesala, W. Hong, Q. Quan, M. D. Lukin, and M. Lončar, "High quality-factor optical nanocavities in bulk single-crystal diamond," Nat. Commun. **5**, 5718 (2014).
[147]M. J. Burek, J. D. Cohen, S. M. Meenehan, N. El-Sawah, C. Chia, T. Ruelle, S. Meesala, J. Rochman, H. A. Atikian, M. Markham, D. J. Twitchen, M. D. Lukin, O. Painter, and M. Lončar, "Diamond optomechanical crystals," Optica **3**, 1404 (2016).
[148]L. Robledo, H. Bernien, I. van Weperen, and R. Hanson, "Control and coherence of the optical transition of single nitrogen vacancy centers in diamond," Phys. Rev. Lett. **105**, 177403 (2010).
[149]C. Santori, P. E. Barclay, K.-M. C. Fu, R. G. Beausoleil, S. Spillane, and M. Fisch, "Nanophotonics for quantum optics using nitrogen-vacancy centers in diamond," Nanotechnology **21**, 274008 (2010).
[150]U. Jantzen, A. B. Kurz, D. S. Rudnicki, C. Schäfermeier, K. D. Jahnke, U. L. Andersen, V. A. Davydov, V. N. Agafonov, A. Kubanek, L. J. Rogers, and F. Jelezko, "Nanodiamonds carrying silicon-vacancy quantum emitters with almost lifetime-limited linewidths," New J. Phys. **18**, 073036 (2016).
[151]J. Borregaard, A. S. Sørensen, and P. Lodahl, "Quantum networks with deterministic spin–photon interfaces," Adv. Quantum Technol. **2**, 1800091 (2019).
[152]B. J. Hausmann, B. Shields, Q. Quan, P. Maletinsky, M. McCutcheon, J. T. Choy, T. M. Babinec, A. Kubanek, A. Yacoby, M. D. Lukin, and M. Lončar, "Integrated diamond networks for quantum nanophotonics," Nano Lett. **12**, 1578–1582 (2012).
[153]S. I. Bogdanov, O. A. Makarova, X. Xu, Z. O. Martin, A. S. Lagutchev, M. Olinde, D. Shah, S. N. Chowdhury, A. R. Gabidullin, I. A. Ryzhikov, I. A. Rodionov, A. V. Kildishev, S. I. Bozhevolnyi, A. Boltasseva, V. M. Shalaev, and J. B. Khurgin, "Ultrafast quantum photonics enabled by coupling plasmonic nanocavities to strongly radiative antennas," Optica **7**, 463 (2020).
[154]J. Wolters, A. W. Schell, G. Kewes, N. Nüsse, M. Schoengen, H. Döscher, T. Hannappel, B. Löchel, M. Barth, and O. Benson, "Enhancement of the zero phonon line emission from a single nitrogen vacancy center in a nanodiamond via coupling to a photonic crystal cavity," Appl. Phys. Lett. **97**, 141108 (2010).
[155]T. Van Der Sar, J. Hagemeier, W. Pfaff, E. C. Heeres, S. M. Thon, H. Kim, P. M. Petroff, T. H. Oosterkamp, D. Bouwmeester, and R. Hanson, "Deterministic nanoassembly of a coupled quantum emitter-photonic crystal cavity system," Appl. Phys. Lett. **98**, 193103 (2011).
[156]K. G. Fehler, A. P. Ovvyan, N. Gruhler, W. H. P. Pernice, and A. Kubanek, "Efficient coupling of an ensemble of nitrogen vacancy center to the mode of a high-Q, Si_3N_4 photonic crystal cavity," ACS Nano **13**, 6891–6898 (2019).
[157]K. G. Fehler, A. P. Ovvyan, L. Antoniuk, N. Lettner, N. Gruhler, V. A. Davydov, V. N. Agafonov, W. H. Pernice, and A. Kubanek, "Purcell-enhanced emission from individual SiV-center in nanodiamonds coupled to a Si_3N_4-based, photonic crystal cavity," Nanophotonics **9**, 3655–3662 (2020).
[158]D. Englund, B. Shields, K. Rivoire, F. Hatami, J. Vučković, H. Park, and M. D. Lukin, "Deterministic coupling of a single nitrogen vacancy center to a photonic crystal cavity," Nano Lett. **10**, 3922–3926 (2010).
[159]P. E. Barclay, K. M. C. Fu, C. Santori, A. Faraon, and R. G. Beausoleil, "Hybrid nanocavity resonant enhancement of color center emission in diamond," Phys. Rev. X **1**, 011007 (2011).
[160]M. Gould, E. R. Schmidgall, S. Dadgostar, F. Hatami, and K. M. C. Fu, "Efficient extraction of zero-phonon-Line photons from single nitrogen-vacancy centers in an integrated GaP-on-diamond platform," Phys. Rev. Appl. **6**, 011001 (2016).
[161]R. Albrecht, A. Bommer, C. Deutsch, J. Reichel, and C. Becher, "Coupling of a single nitrogen-vacancy center in diamond to a fiber-based microcavity," Phys. Rev. Lett. **110**, 243602 (2013).

[162]H. Kaupp, C. Deutsch, H. C. Chang, J. Reichel, T. W. Hänsch, and D. Hunger, "Scaling laws of the cavity enhancement for nitrogen-vacancy centers in diamond," Phys. Rev. A **88**, 053812 (2013).
[163]R. Albrecht, A. Bommer, C. Pauly, F. Mücklich, A. W. Schell, P. Engel, T. Schröder, O. Benson, J. Reichel, and C. Becher, "Narrow-band single photon emission at room temperature based on a single nitrogen-vacancy center coupled to an all-fiber-cavity," Appl. Phys. Lett. **105**, 073113 (2014).
[164]S. Johnson, P. R. Dolan, T. Grange, A. A. P. Trichet, G. Hornecker, Y. C. Chen, L. Weng, G. M. Hughes, A. A.. R. Watt, A. Auffeves, and J. M. Smith, "Tunable cavity coupling of the zero phonon line of a nitrogen-vacancy defect in diamond," New J. Phys. **17**, 122003 (2015).
[165]H. Kaupp, T. Hümmer, M. Mader, B. Schlederer, J. Benedikter, P. Haeusser, H.-C. Chang, H. Fedder, T. W. Hänsch, and D. Hunger, "Purcell-enhanced single-photon emission from nitrogen-vacancy centers coupled to a tunable microcavity," Phys. Rev. Appl. **6**, 054010 (2016).
[166]J. Benedikter, H. Kaupp, T. Hümmer, Y. Liang, A. Bommer, C. Becher, A. Krueger, J. M. Smith, T. W. Hänsch, and D. Hunger, "Cavity-enhanced single-photon source based on the silicon-vacancy center in diamond," Phys. Rev. Appl. **7**, 024031 (2017).
[167]S. Häußler, J. Benedikter, K. Bray, B. Regan, A. Dietrich, J. Twamley, I. Aharonovich, D. Hunger, and A. Kubanek, "Diamond photonics platform based on silicon vacancy centers in a single-crystal diamond membrane and a fiber cavity," Phys. Rev. B **99**, 165310 (2019).
[168]M. Salz, Y. Herrmann, A. Nadarajah, A. Stahl, M. Hettrich, A. Stacey, S. Prawer, D. Hunger, and F. Schmidt-Kaler, "Cryogenic platform for coupling color centers in diamond membranes to a fiber-based microcavity," Appl. Phys. B **126**, 131 (2020).
[169]B. J. M. Hausmann, B. J. Shields, Q. Quan, Y. Chu, N. P. de Leon, R. Evans, M. J. Burek, A. S. Zibrov, M. Markham, D. J. Twitchen, H. Park, M. D. Lukin, and M. Lončar, "Coupling of NV centers to photonic crystal nanobeams in diamond," Nano Lett. **13**, 5791–5796 (2013).
[170]L. Li, T. Schröder, E. H. Chen, M. Walsh, I. Bayn, J. Goldstein, O. Gaathon, M. E. Trusheim, M. Lu, J. Mower, M. Cotlet, M. L. Markham, D. J. Twitchen, and D. Englund, "Coherent spin control of a nanocavity-enhanced qubit in diamond," Nat. Commun. **6**, 6173 (2015).
[171]J. Riedrich-Möller, S. Pezzagna, J. Meijer, C. Pauly, F. Mücklich, M. Markham, A. M. Edmonds, and C. Becher, "Nanoimplantation and Purcell enhancement of single nitrogen-vacancy centers in photonic crystal cavities in diamond," Appl. Phys. Lett. **106**, 221103 (2015).
[172]T. Schröder, M. Walsh, J. Zheng, S. Mouradian, L. Li, G. Malladi, H. Bakhru, M. Lu, A. Stein, M. Heuck, and D. Englund, "Scalable fabrication of coupled NV center-photonic crystal cavity systems by self-aligned N ion implantation," Opt. Mater. Express **7**, 682–686 (2017).
[173]T. Jung, J. Görlitz, B. Kambs, C. Pauly, N. Raatz, R. Nelz, E. Neu, A. M. Edmonds, M. Markham, F. Mücklich, J. Meijer, and C. Becher, "Spin measurements of NV centers coupled to a photonic crystal cavity," APL Photonics **4**, 120803 (2019).
[174]C. Dory, D. Vercruysse, K. Y. Yang, N. V. Sapra, A. E. Rugar, S. Sun, D. M. Lukin, A. Y. Piggott, J. L. Zhang, M. Radulaski, K. G. Lagoudakis, L. Su, and J. Vučković, "Inverse-designed diamond photonics," Nat. Commun. **10**, 3309 (2019).
[175]P. Rath, S. Khasminskaya, C. Nebel, C. Wild, and W. H. Pernice, "Grating-assisted coupling to nanophotonic circuits in microcrystalline diamond thin films," Beilstein J. Nanotechnol. **4**, 300–305 (2013).
[176]B. Khanaliloo, H. Jayakumar, A. C. Hryciw, D. P. Lake, H. Kaviani, and P. E. Barclay, "Single-crystal diamond nanobeam waveguide optomechanics," Phys. Rev. X **5**, 041051 (2015).
[177]M. Mitchell, D. P. Lake, and P. E. Barclay, "Realizing $Q > 300\,000$ in diamond microdisks for optomechanics via etch optimization," APL Photonics **4**, 016101 (2019).
[178]M. J. Burek, C. Meuwly, R. E. Evans, M. K. Bhaskar, A. Sipahigil, S. Meesala, B. MacHielse, D. D. Sukachev, C. T. Nguyen, J. L. Pacheco, E. Bielejec, M. D. Lukin, and M. Lončar, "Fiber-coupled diamond quantum nanophotonic interface," Phys. Rev. Appl. **8**, 024026 (2017).
[179]D. Bluvstein, Z. Zhang, and A. C. Jayich, "Identifying and mitigating charge instabilities in shallow diamond nitrogen-vacancy centers," Phys. Rev. Lett. **122**, 76101 (2019).
[180]S. Sangtawesin, B. L. Dwyer, S. Srinivasan, J. J. Allred, L. V. Rodgers, K. De Greve, A. Stacey, N. Dontschuk, K. M. O'Donnell, D. Hu, D. A. Evans, C. Jaye, D. A. Fischer, M. L. Markham, D. J. Twitchen, H. Park, M. D. Lukin, and N. P. de Leon, "Origins of diamond surface noise probed by correlating single-spin measurements with surface spectroscopy," Phys. Rev. X **9**, 031052 (2019).
[181]H. F. Fotso, A. E. Feiguin, D. D. Awschalom, and V. V. Dobrovitski, "Suppressing spectral diffusion of emitted photons with optical pulses," Phys. Rev. Lett. **116**, 033603 (2016).
[182]E. Janitz, M. Ruf, M. Dimock, A. Bourassa, J. Sankey, and L. Childress, "Fabry–Pérot microcavity for diamond-based photonics," Phys. Rev. A **92**, 043844 (2015).
[183]Y. Fontana, R. Zifkin, E. Janitz, C. D. Rodríguez Rosenblueth, and L. Childress, "A mechanically stable and tunable cryogenic Fabry–Pérot microcavity," Rev. Sci. Instrum. **92**, 053906 (2021).
[184]I. Lekavicius, T. Oo, and H. Wang, "Diamond lamb wave spin-mechanical resonators with optically coherent nitrogen vacancy centers," J. Appl. Phys. **126**, 214301 (2019).
[185]M. Kasperczyk, J. A. Zuber, A. Barfuss, J. Kölbl, V. Yurgens, S. Flågan, T. Jakubczyk, B. Shields, R. J. Warburton, and P. Maletinsky, "Statistically modeling optical linewidths of nitrogen vacancy centers in microstructures," Phys. Rev. B **102**, 075312 (2020).
[186]V. Yurgens, J. A. Zuber, S. Flågan, M. De Luca, B. J. Shields, I. Zardo, P. Maletinsky, R. J. Warburton, and T. Jakubczyk, "Low-charge-noise nitrogen-vacancy centers in diamond created using laser writing with a solid-immersion lens," ACS Photonics **8**, 1726–1734 (2021).
[187]Y.-C. Chen, B. Griffiths, L. Weng, S. S. Nicley, S. N. Ishmael, Y. Lekhai, S. Johnson, C. J. Stephen, B. L. Green, G. W. Morley, M. E. Newton, M. J. Booth, P. S. Salter, and J. M. Smith, "Laser writing of individual nitrogen-vacancy defects in diamond with near-unity yield," Optica **6**, 662 (2019).
[188]S. B. van Dam, M. Walsh, M. J. Degen, E. Bersin, S. L. Mouradian, A. Galiullin, M. Ruf, M. IJspeert, T. H. Taminiau, R. Hanson, and D. R. Englund, "Optical coherence of diamond nitrogen-vacancy centers formed by ion implantation and annealing," Phys. Rev. B **99**, 161203 (2019).
[189]Y. Chu, N. de Leon, B. Shields, B. Hausmann, R. Evans, E. Togan, M. J. Burek, M. Markham, A. Stacey, A. Zibrov, A. Yacoby, D. Twitchen, M. Loncar, H. Park, P. Maletinsky, and M. Lukin, "Coherent optical transitions in implanted nitrogen vacancy centers," Nano Lett. **14**, 1982–1986 (2014).
[190]F. Rozpędek, R. Yehia, K. Goodenough, M. Ruf, P. C. Humphreys, R. Hanson, S. Wehner, and D. Elkouss, "Near-term quantum-repeater experiments with nitrogen-vacancy centers: Overcoming the limitations of direct transmission," Phys. Rev. A **99**, 052330 (2019).
[191]G. Murta, S. B. van Dam, J. Ribeiro, R. Hanson, and S. Wehner, "Towards a realization of device-independent quantum key distribution," Q. Sci. Technol. **4**, 035011 (2019).
[192]A. Sipahigil, K. D. Jahnke, L. J. Rogers, T. Teraji, J. Isoya, A. S. Zibrov, F. Jelezko, and M. D. Lukin, "Indistinguishable photons from separated silicon-vacancy centers in diamond," Phys. Rev. Lett. **113**, 113602 (2014).
[193]R. E. Evans, A. Sipahigil, D. D. Sukachev, A. S. Zibrov, and M. D. Lukin, "Narrow-linewidth homogeneous optical emitters in diamond nanostructures via silicon ion implantation," Phys. Rev. Appl. **5**, 044010 (2016).
[194]T. Múller, C. Hepp, B. Pingault, E. Neu, S. Gsell, M. Schreck, H. Sternschulte, D. Steinmüller-Nethl, C. Becher, and M. Atatúre, "Optical signatures of silicon-vacancy spins in diamond," Nat. Commun. **5**, 3328 (2014).
[195]S. Maity, L. Shao, Y.-I. Sohn, S. Meesala, B. Machielse, E. Bielejec, M. Markham, and M. Lončar, "Spectral alignment of single-photon emitters in diamond using strain gradient," Phys. Rev. Appl. **10**, 024050 (2018).
[196]S. Sun, J. L. Zhang, K. A. Fischer, M. J. Burek, C. Dory, K. G. Lagoudakis, Y.-K. Tzeng, M. Radulaski, Y. Kelaita, A. Safavi-Naeini, Z.-X. Shen, N. A. Melosh, S. Chu, M. Lončar, and J. Vučković, "Cavity-enhanced Raman emission from a single color center in a solid," Phys. Rev. Lett. **121**, 083601 (2018).

[197]A. E. Rugar, H. Lu, C. Dory, S. Sun, P. J. McQuade, Z. X. Shen, N. A. Melosh, and J. Vučković, "Generation of tin-vacancy centers in diamond via shallow ion implantation and subsequent diamond overgrowth," Nano Lett. **20**, 1614–1619 (2020).
[198]C. A. McLellan, B. A. Myers, S. Kraemer, K. Ohno, D. D. Awschalom, and A. C. Bleszynski Jayich, "Patterned formation of highly coherent nitrogen-vacancy centers using a focused electron irradiation technique," Nano Lett. **16**, 2450–2454 (2016).
[199]A. T. Collins, "The fermi level in diamond," J. Phys.: Condens. Matter **14**, 3743–3750 (2002).
[200]T. Murai, T. Makino, H. Kato, M. Shimizu, T. Murooka, E. D. Herbschleb, Y. Doi, H. Morishita, M. Fujiwara, M. Hatano, S. Yamasaki, and N. Mizuochi, "Engineering of Fermi level by NiN diamond junction for control of charge states of NV centers," Appl. Phys. Lett. **112**, 111903 (2018).
[201]T. Lúhmann, R. John, R. Wunderlich, J. Meijer, and S. Pezzagna, "Coulomb-driven single defect engineering for scalable qubits and spin sensors in diamond," Nat. Commun. **10**, 4956 (2019).
[202]M. Schreck, S. Gsell, R. Brescia, and M. Fischer, "Ion bombardment induced buried lateral growth: The key mechanism for the synthesis of single crystal diamond wafers," Sci. Rep. **7**, 44462 (2017).
[203]R. Nelz, J. Görlitz, D. Herrmann, A. Slablab, M. Challier, M. Radtke, M. Fischer, S. Gsell, M. Schreck, C. Becher, and E. Neu, "Toward wafer-scale diamond nano- and quantum technologies," APL Mater. **7**, 011108 (2019).
[204]N. R. Parikh, J. D. Hunn, E. McGucken, M. L. Swanson, C. W. White, R. A. Rudder, D. P. Malta, J. B. Posthill, and R. J. Markunas, "Single-crystal diamond plate liftoff achieved by ion implantation and subsequent annealing," Appl. Phys. Lett. **61**, 3124–3126 (1992).
[205]B. A. Fairchild, P. Olivero, S. Rubanov, A. D. Greentree, F. Waldermann, R. A. Taylor, I. Walmsley, J. M. Smith, S. Huntington, B. C. Gibson, D. N. Jamieson, and S. Prawer, "Fabrication of ultrathin single-crystal diamond membranes," Adv. Mater. **20**, 4793–4798 (2008).
[206]O. Gaathon, J. S. Hodges, E. H. Chen, L. Li, S. Bakhru, H. Bakhru, D. Englund, and R. M. Osgood, "Planar fabrication of arrays of ion-exfoliated single-crystal-diamond membranes with nitrogen-vacancy color centers," Opt. Mater. **35**, 361–365 (2013).
[207]J. C. Lee, D. O. Bracher, S. Cui, K. Ohno, C. A. McLellan, X. Zhang, P. Andrich, B. Alemán, K. J. Russell, A. P. Magyar, I. Aharonovich, A. Bleszynski Jayich, D. Awschalom, and E. L. Hu, "Deterministic coupling of delta-doped nitrogen vacancy centers to a nanobeam photonic crystal cavity," Appl. Phys. Lett. **105**, 261101 (2014).
[208]A. H. Piracha, K. Ganesan, D. W. M. Lau, A. Stacey, L. P. McGuinness, S. Tomljenovic-Hanic, and S. Prawer, "Scalable fabrication of high-quality, ultra-thin single crystal diamond membrane windows," Nanoscale **8**, 6860–6865 (2016).
[209]A. H. Piracha, P. Rath, K. Ganesan, S. Kúhn, W. H. Pernice, and S. Prawer, "Scalable fabrication of integrated nanophotonic circuits on arrays of thin single crystal diamond membrane windows," Nano Lett. **16**, 3341–3347 (2016).
[210]J. V. Cady, O. Michel, K. W. Lee, R. N. Patel, C. J. Sarabalis, A. H. Safavi-Naeini, and A. C. Bleszynski Jayich, "Diamond optomechanical crystals with embedded nitrogen-vacancy centers," Q. Sci. Technol. **4**, 024009 (2019).
[211]I. Bayn, S. Mouradian, L. Li, J. A. Goldstein, T. Schröder, J. Zheng, E. H. Chen, O. Gaathon, M. Lu, A. Stein, C. A. Ruggiero, J. Salzman, R. Kalish, and D. Englund, "Fabrication of triangular nanobeam waveguide networks in bulk diamond using single-crystal silicon hard masks," Appl. Phys. Lett. **105**, 211101 (2014).
[212]H. A. Atikian, P. Latawiec, M. J. Burek, Y.-I. Sohn, S. Meesala, N. Gravel, A. B. Kouki, and M. Lončar, "Freestanding nanostructures via reactive ion beam angled etching," APL Photonics **2**, 051301 (2017).
[213]J. L. Zhang, S. Sun, M. J. Burek, C. Dory, Y.-K. Tzeng, K. A. Fischer, Y. Kelaita, K. G. Lagoudakis, M. Radulaski, Z.-X. Shen, N. A. Melosh, S. Chu, M. Lončar, and J. Vučković, "Strongly cavity-enhanced spontaneous emission from silicon-vacancy centers in diamond," Nano Lett. **18**, 1360–1365 (2018).
[214]B. Khanaliloo, M. Mitchell, A. C. Hryciw, and P. E. Barclay, "High-Q/V monolithic diamond microdisks fabricated with quasi-isotropic etching," Nano Lett. **15**, 5131–5136 (2015).
[215]B. Khanaliloo, H. Jayakumar, A. C. Hryciw, D. P. Lake, H. Kaviani, and P. E. Barclay, "Single-crystal diamond nanobeam waveguide optomechanics," Phys. Rev. X **5**, 041051 (2015).
[216]S. Mouradian, N. H. Wan, T. Schröder, and D. Englund, "Rectangular photonic crystal nanobeam cavities in bulk diamond," Appl. Phys. Lett. **111**, 021103 (2017).
[217]N. H. Wan, S. Mouradian, and D. Englund, "Two-dimensional photonic crystal slab nanocavities on bulk single-crystal diamond," Appl. Phys. Lett. **112**, 141102 (2018).
[218]J. Zheng, B. Lienhard, G. Doerk, M. Cotlet, E. Bersin, H. S. Kim, Y.-C. Byun, C.-Y. Nam, J. Kim, C. T. Black, and D. Englund, "Top-down fabrication of high-uniformity nanodiamonds by self-assembled block copolymer masks," Sci. Rep. **9**, 6914 (2019).
[219]S. Mosor, J. Hendrickson, B. C. Richards, J. Sweet, G. Khitrova, H. M. Gibbs, T. Yoshie, A. Scherer, O. B. Shchekin, and D. G. Deppe, "Scanning a photonic crystal slab nanocavity by condensation of xenon," Appl. Phys. Lett. **87**, 141105 (2005).
[220]Y. Lee, E. Bersin, A. Dahlberg, S. Wehner, and D. Englund, "A quantum router architecture for high-fidelity entanglement flows in quantum networks," arXiv:2005.01852 (2020).
[221]M. Pant, H. Krovi, D. Towsley, L. Tassiulas, L. Jiang, P. Basu, D. Englund, and S. Guha, "Routing entanglement in the quantum internet," npj Q. Inform. **5**, 1–9 (2019).
[222]A. Tchebotareva, S. L. Hermans, P. C. Humphreys, D. Voigt, P. J. Harmsma, L. K. Cheng, A. L. Verlaan, N. Dijkhuizen, W. de Jong, A. Dréau, and R. Hanson, "Entanglement between a diamond spin qubit and a photonic time-bin qubit at telecom wavelength," Phys. Rev. Lett. **123**, 063601 (2019).
[223]V. Krutyanskiy, M. Meraner, J. Schupp, V. Krcmarsky, H. Hainzer, and B. P. Lanyon, "Light-matter entanglement over 50 km of optical fibre," npj Q. Inform. **5**, 72 (2019).
[224]M. Bock, P. Eich, S. Kucera, M. Kreis, A. Lenhard, C. Becher, and J. Eschner, "High-fidelity entanglement between a trapped ion and a telecom photon via quantum frequency conversion," Nat. Commun. **9**, 1998 (2018).
[225]R. Ikuta, T. Kobayashi, T. Kawakami, S. Miki, M. Yabuno, T. Yamashita, H. Terai, M. Koashi, T. Mukai, T. Yamamoto, and N. Imoto, "Polarization insensitive frequency conversion for an atom-photon entanglement distribution via a telecom network," Nat. Commun. **9**, 1997 (2018).
[226]Y. Yu, F. Ma, X. Y. Luo, B. Jing, P. F. Sun, R. Z. Fang, C. W. Yang, H. Liu, M. Y. Zheng, X. P. Xie, W. J. Zhang, L. X. You, Z. Wang, T. Y. Chen, Q. Zhang, X. H. Bao, and J. W. Pan, "Entanglement of two quantum memories via fibres over dozens of kilometres," Nature **578**, 240–245 (2020).
[227]K. De Greve, L. Yu, P. L. McMahon, J. S. Pelc, C. M. Natarajan, N. Y. Kim, E. Abe, S. Maier, C. Schneider, M. Kamp, S. Höfling, R. H. Hadfield, A. Forchel, M. M. Fejer, and Y. Yamamoto, "Quantum-dot spin-photon entanglement via frequency downconversion to telecom wavelength," Nature **491**, 421–425 (2012).
[228]I. Pogorelov, T. Feldker, C. D. Marciniak, L. Postler, G. Jacob, O. Krieglsteiner, V. Podlesnic, M. Meth, V. Negnevitsky, M. Stadler, B. Höfer, C. Wächter, K. Lakhmanskiy, R. Blatt, P. Schindler, and T. Monz, "Compact ion-trap quantum computing demonstrator," PRX Quantum **2**, 020343 (2021).
[229]S. Muralidharan, L. Li, J. Kim, N. Lütkenhaus, M. D. Lukin, and L. Jiang, "Optimal architectures for long distance quantum communication," Sci. Rep. **6**, 20463 (2016).
[230]W. Bogaerts, D. Pérez, J. Capmany, D. A. B. Miller, J. Poon, D. Englund, F. Morichetti, and A. Melloni, "Programmable photonic circuits," Nature **586**, 207–216 (2020).
[231]N. C. Harris, J. Carolan, D. Bunandar, M. Prabhu, M. Hochberg, T. Baehr-Jones, M. L. Fanto, A. M. Smith, C. C. Tison, P. M. Alsing, and D. Englund, "Linear programmable nanophotonic processors," Optica **5**, 1623 (2018).
[232]D. J. Blumenthal, R. Heideman, D. Geuzebroek, A. Leinse, and C. Roeloffzen, "silicon nitride in Silicon photonics," Proc. IEEE **106**, 2209–2231 (2018).

[233]D. Zhu, L. Shao, M. Yu, R. Cheng, B. Desiatov, C. J. Xin, Y. Hu, J. Holzgrafe, S. Ghosh, A. Shams-Ansari, E. Puma, N. Sinclair, C. Reimer, M. Zhang, and M. Lončar, "Integrated photonics on thin-film lithium niobate," Adv. Opt. Photonics **13**, 242 (2021).
[234]C. Sun, M. T. Wade, Y. Lee, J. S. Orcutt, L. Alloatti, M. S. Georgas, A. S. Waterman, J. M. Shainline, R. R. Avizienis, S. Lin, B. R. Moss, R. Kumar, F. Pavanello, A. H. Atabaki, H. M. Cook, A. J. Ou, J. C. Leu, Y. H. Chen, K. Asanović, R. J. Ram, M. A. Popović, and V. M. Stojanović, "Single-chip microprocessor that communicates directly using light," Nature **528**, 534–538 (2015).
[235]A. H. Atabaki, S. Moazeni, F. Pavanello, H. Gevorgyan, J. Notaros, L. Alloatti, M. T. Wade, C. Sun, S. A. Kruger, H. Meng, K. Al Qubaisi, I. Wang, B. Zhang, A. Khilo, C. V. Baiocco, M. A. Popović, V. M. Stojanović, and R. J. Ram, "Integrating photonics with silicon nanoelectronics for the next generation of systems on a chip," Nature **556**, 349–354 (2018).
[236]G. Wetzstein, A. Ozcan, S. Gigan, S. Fan, D. Englund, M. Soljačić, C. Denz, D. A. B. Miller, and D. Psaltis, "Inference in artificial intelligence with deep optics and photonics," Nature **588**, 39–47 (2020).
[237]B. J. Shastri, A. N. Tait, T. Ferreira de Lima, W. H. P. Pernice, H. Bhaskaran, C. D. Wright, and P. R. Prucnal, "Photonics for artificial intelligence and neuromorphic computing," Nat. Photonics **15**, 102–114 (2021).
[238]J. Wang, F. Sciarrino, A. Laing, and M. G. Thompson, "Integrated photonic quantum technologies," Nat. Photonics **14**, 273–284 (2020).
[239]C. Wang, C. Langrock, A. Marandi, M. Jankowski, M. Zhang, B. Desiatov, M. M. Fejer, and M. Lončar, "Ultrahigh-efficiency wavelength conversion in nanophotonic periodically poled lithium niobate waveguides," Optica **5**, 1438 (2018).
[240]B. J. M. Hausmann, I. Bulu, V. Venkataraman, P. Deotare, and M. Lončar, "Diamond nonlinear photonics," Nat. Photonics **8**, 369–374 (2014).
[241]J. Kim, S. Aghaeimeibodi, J. Carolan, D. Englund, and E. Waks, "Hybrid integration methods for on-chip quantum photonics," Optica **7**, 291 (2020).
[242]A. W. Elshaari, W. Pernice, K. Srinivasan, O. Benson, and V. Zwiller, "Hybrid integrated quantum photonic circuits," Nat. Photonics **14**, 285–298 (2020).
[243]T. Komljenovic, D. Huang, P. Pintus, M. A. Tran, M. L. Davenport, and J. E. Bowers, "Photonic integrated circuits using heterogeneous integration on silicon," Proc. IEEE **106**, 2246–2257 (2018).
[244]F. Najafi, J. Mower, N. C. Harris, F. Bellei, A. Dane, C. Lee, X. Hu, P. Kharel, F. Marsili, S. Assefa, K. K. Berggren, and D. Englund, "On-chip detection of non-classical light by scalable integration of single-photon detectors," Nat. Commun. **6**, 5873 (2015).
[245]E. Bersin, M. Walsh, S. L. Mouradian, M. E. Trusheim, T. Schröder, and D. Englund, "Individual control and readout of qubits in a sub-diffraction volume," npj Q. Inform. **5**, 38 (2019).
[246]S. Chen, M. Raha, C. M. Phenicie, S. Ourari, and J. D. Thompson, "Parallel single-shot measurement and coherent control of solid-state spins below the diffraction limit," Science **370**, 592–595 (2020).
[247]D. Kim, M. I. Ibrahim, C. Foy, M. E. Trusheim, R. Han, and D. R. Englund, "A CMOS-integrated quantum sensor based on nitrogen-vacancy centres," Nat. Electron. **2**, 284–289 (2019).
[248]G. Reithmaier, M. Kaniber, F. Flassig, S. Lichtmannecker, K. Müller, A. Andrejew, J. Vučković, R. Gross, and J. J. Finley, "On-chip generation, routing, and detection of resonance fluorescence," Nano Lett. **15**, 5208–5213 (2015).
[249]M. Schwartz, E. Schmidt, U. Rengstl, F. Hornung, S. Hepp, S. L. Portalupi, K. Llin, M. Jetter, M. Siegel, and P. Michler, "Fully on-chip single-photon Hanbury–Brown and Twiss experiment on a monolithic semiconductor–superconductor platform," Nano Lett. **18**, 6892–6897 (2018).
[250]S. Gyger, J. Zichi, L. Schweickert, A. W. Elshaari, S. Steinhauer, S. F. Covre da Silva, A. Rastelli, V. Zwiller, K. D. Jöns, and C. Errando-Herranz, "Reconfigurable photonics with on-chip single-photon detectors," Nat. Commun. **12**, 1408 (2021).
[251]X. Guo, C.-L. Zou, H. Jung, and H. X. Tang, "On-chip strong coupling and efficient frequency conversion between telecom and visible optical modes," Phys. Rev. Lett. **117**, 123902 (2016).
[252]M. Jankowski, C. Langrock, B. Desiatov, A. Marandi, C. Wang, M. Zhang, C. R. Phillips, M. Lončar, and M. M. Fejer, "Ultrabroadband nonlinear optics in nanophotonic periodically poled lithium niobate waveguides," Optica **7**, 40 (2020).
[253]Y. Hu, M. Yu, D. Zhu, N. Sinclair, A. Shams-Ansari, L. Shao, J. Holzgrafe, E. Puma, M. Zhang, and M. Loncar, "Reconfigurable electro-optic frequency shifter," arXiv:2005.09621 (2020).
[254]C. H. Bennett, G. Brassard, S. Popescu, B. Schumacher, J. A. Smolin, and W. K. Wootters, "Purification of noisy entanglement and faithful teleportation via noisy channels," Phys. Rev. Lett. **76**, 722–725 (1996).
[255]D. Deutsch, A. Ekert, R. Jozsa, C. Macchiavello, S. Popescu, and A. Sanpera, "quantum privacy amplification and the security of Quantum cryptography over noisy channels," Phys. Rev. Lett. **77**, 2818–2821 (1996).
[256]L. Jiang, J. S. Hodges, J. R. Maze, P. Maurer, J. M. Taylor, D. G. Cory, P. R. Hemmer, R. L. Walsworth, A. Yacoby, A. S. Zibrov, and M. D. Lukin, "Repetitive readout of a single electronic spin via quantum logic with nuclear spin ancillae," Science **326**, 267–272 (2009).
[257]D. Poulin, "Optimal and efficient decoding of concatenated quantum block codes," Phys. Rev. A **74**, 052333 (2006).
[258]J. Borregaard, H. Pichler, T. Schröder, M. D. Lukin, P. Lodahl, and A. S. Sørensen, "One-way quantum repeater based on near-deterministic photon-emitter interfaces," Phys. Rev. X **10**, 021071 (2020).
[259]A. Dahlberg, M. Skrzypczyk, T. Coopmans, L. Wubben, F. Rozpędek, M. Pompili, A. Stolk, P. Pawełczak, R. Knegjens, J. de Oliveira Filho, R. Hanson, and S. Wehner, "A link layer protocol for quantum networks," in *Proceedings of the ACM Special Interest Group on Data Communication* (ACM, New York, 2019), pp. 159–173.
[260]A. Pirker and W. Dür, "A quantum network stack and protocols for reliable entanglement-based networks," New J. Phys. **21**, 033003 (2019).
[261]D. Cuomo, M. Caleffi, and A. S. Cacciapuoti, "Towards a distributed quantum computing ecosystem," IET Q. Commun. **1**, 3–8 (2020).
[262]A. Broadbent, J. Fitzsimons, and E. Kashefi, "Universal blind quantum computation," in *2009 50th Annual IEEE Symposium on Foundations of Computer Science* (IEEE, 2009), pp. 517–526.
[263]J. S. Hodges, N. Y. Yao, D. Maclaurin, C. Rastogi, M. D. Lukin, and D. Englund, "Timekeeping with electron spin states in diamond," Phys. Rev. A **87**, 032118 (2013).